



## Assessment of the impacts of cloud chemistry on surface SO<sub>2</sub> and sulfate levels in typical regions of China

Jianyan Lu<sup>1</sup>, Sunling Gong<sup>1,5</sup>, Jian Zhang<sup>1</sup>, Jianmin Chen<sup>2,3,4</sup>, Lei Zhang<sup>1</sup>, and Chunhong Zhou<sup>1</sup>

<sup>1</sup>State Key Laboratory of Severe Weather, Key Laboratory of Atmospheric Chemistry of CMA, Institute of Atmospheric Composition, Chinese Academy of Meteorological Sciences, Beijing 100081, China

<sup>2</sup>Shanghai Key Laboratory of Atmospheric Particle Pollution and Prevention (LAP3), Department of Environmental Science and Engineering, Fudan Tyndall Centre, Institute of Atmospheric Sciences, Fudan University, Shanghai, China

<sup>3</sup>Center for Excellence in Urban Atmospheric Environment, Institute of Urban Environment, Chinese Academy of Science, Xiamen, China

<sup>4</sup>Shanghai Institute of Eco-Chongming (SIEC), No. 3663 Northern Zhongshan Road, Shanghai 200062, China

<sup>5</sup>National Observation and Research Station of Coastal Ecological Environments in Macao, Macao Environmental Research Institute, Macao University of Science and Technology, Macao SAR 999078, China

**Correspondence:** Sunling Gong (gongsl@cma.gov.cn) and Chunhong Zhou (zhouch@cma.gov.cn)

Received: 21 March 2023 – Discussion started: 24 March 2023

Revised: 31 May 2023 – Accepted: 2 June 2023 – Published: 19 July 2023

**Abstract.** A regional online chemical weather model, Weather Research and Forecasting (WRF)/China Meteorological Administration Unified Atmospheric Chemistry Environment (CUACE), is used to assess the contributions of cloud chemistry to the SO<sub>2</sub> and sulfate levels in typical regions of China. Upon comparison with several time series of in situ cloud chemical observations on Mountain Tai in Shandong Province of China, the CUACE cloud chemistry scheme is found to reasonably reproduce the observed cloud consumption of H<sub>2</sub>O<sub>2</sub>, O<sub>3</sub>, and SO<sub>2</sub> and the production of sulfate, and it is consequently used in the regional assessment of a heavy pollution episode and monthly average of December 2016. During the cloudy period in the heavy pollution episode, sulfate production increased by 60 %–95 % and SO<sub>2</sub> production reduced by over 80 %. The cloud chemistry mainly affects the middle and lower troposphere below 5 km as well as within the boundary layer, and it contributes significantly to the SO<sub>2</sub> reduction and sulfate production in central-east China. Among these four typical regions in China, the Sichuan Basin (SCB) is the most affected by the cloud chemistry, with an average SO<sub>2</sub> abatement of about 1.0–10.0 ppb and sulfate increase of about 10.0–70.0 μg m<sup>-3</sup>, followed by the Yangtze River Delta (YRD) and the southeast of the North China Plain (NCP), where SO<sub>2</sub> abatement is about 1.0–5.0 ppb and sulfate increase is about 10.0–30.0 μg m<sup>-3</sup>. However, the cloud chemistry contributions to the Pearl River Delta (PRD) and the northwest of the NCP are not significant due to lighter pollution and less water vapor than the other regions.

## 1 Introduction

Aerosols interact with radiation and clouds, directly or indirectly affecting the atmospheric radiation balance and precipitation, which in turn affects weather and climate (Twomey et al., 1984; Twomey, 1991; Charlson et al., 1992; Ramanathan et al., 2001; Pye et al., 2020). Moreover, large amounts of aerosols dispersed in the atmosphere can reduce visibility and deteriorate air quality (Molina, 2002), which is harmful to human health and ecosystems (Xie et al., 2019; Sielski et al., 2021).

In addition to direct emissions, aerosols are mostly produced secondarily through the oxidation of precursor gases, and one of the important processes is the transformation in clouds. Global cloud coverage of about 21 % to 95 % provides an adequate environment for cloud chemistry processes (Kotarba, 2020; Ravishankara, 1997). As about 90 % of the clouds formed in the atmosphere evaporate without deposition or forming precipitation, large fractions of aerosols formed within clouds can then re-enter the atmosphere (Cafrey et al., 2001; Harris et al., 2013; Lelieveld and Heintzenberg, 1992). Globally, sulfate production from SO<sub>2</sub> oxidation accounts for about 80 % of total sulfate, and more than half of it is produced in clouds (Hung et al., 2018; Faloon et al., 2010; Guo et al., 2012). Ge et al. (2021) found that cloud chemistry processes reduced SO<sub>2</sub> concentrations by 0 %–50 % in most of central-east China in all seasons. Li (2011) found that the average sulfate concentration in cloud water accounted for 53.8 % of the total aerosol concentration at a mountain site. Li (2020) also found that cloud processes effectively reduced atmospheric O<sub>3</sub> and SO<sub>2</sub> concentrations by an average of 19.7 % and 71.2 %, respectively, at Mount Tai.

Multiphase oxidation of SO<sub>2</sub> in aerosol particles in high-humidity environments is one of the main causes of the explosive growth of particulate matter in East Asia haze (Guo et al., 2014; Cheng et al., 2016; Song et al., 2019). From observations and laboratory works, four main pathways were identified for this kind of oxidation of SO<sub>2</sub>, i.e., by H<sub>2</sub>O<sub>2</sub>, O<sub>3</sub>, NO<sub>2</sub>, and transition metal ions (TMIs; Ibusuki and Takeuchi, 1987; Martin and Good, 1991; Alexander et al., 2009; Harris et al., 2013; Cheng et al., 2016; Wang et al., 2016; Wang et al., 2021). Additional pathways of organic peroxides (ROOH; Yao et al., 2019; Wang et al., 2019; Ye et al., 2018; Dovrou et al., 2019), photolysis products of nitrate (*p*NO<sub>3</sub><sup>-</sup>) (Gen et al., 2019b, a), and excited triplet states of photosensitizer molecules (*T*\*; Wang et al., 2020) have also been found recently to be important for multiphase oxidation of SO<sub>2</sub> during very heavy hazy days. Unfortunately, there are still many uncertainties and gaps to put all those pathways into model applications from observational and laboratory studies (Pye et al., 2020; Ravishankara, 1997; Liu et al., 2021). Several regional and global models have tried to include only O<sub>3</sub> and H<sub>2</sub>O<sub>2</sub> in-cloud oxidants in cloud chemistry mechanisms (Park and Jacob, 2003; Tie, 2005; Von Salzen et al., 2000; Chapman et al., 2009; Leighton and Ivanova, 2008; Ivanova

and Leighton, 2008), but only a few models can simulate the pathway of NO<sub>2</sub> or the TMIs of Fe or Mn ions (Chang et al., 1987; Binkowski and Roselle, 2003; Menut et al., 2013; Terrenoire et al., 2015; Ge et al., 2021).

There has been very serious air pollution in central-east China where the four heavy pollution regions of the North China Plain (NCP), Yangtze River Delta (YRD), Sichuan Basin (SCB), and Pearl River Delta (PRD) are located (Yao et al., 2021; Zhang et al., 2012). Although many global and regional models have contained sulfate formation mechanisms by cloud chemistry, few models have assessed its contribution. Especially lacking is a detailed assessment of regional cloud chemistry of sulfate and SO<sub>2</sub> in China. Some models have failed to reproduce SO<sub>2</sub> and sulfate observations, particularly underestimating sulfate and overestimating SO<sub>2</sub> over China (Buchard et al., 2014; Cheng et al., 2016; Hong et al., 2017a; Wei et al., 2019); this is mainly caused by the uncertainties in meteorological conditions (Sun et al., 2016) and emission inventories (Hong et al., 2017b; Sha et al., 2019b), as well as unclear and/or inaccurate physical and chemical mechanisms associated with air pollutants (He and Zhang, 2014; He et al., 2015; Georgiou et al., 2018; Sha et al., 2019a). The inadequate inclusion or lack of cloud chemistry of SO<sub>2</sub> is one of the main causes (Ge et al., 2021). Therefore, it is very important and necessary to quantify the contribution of cloud chemistry in these regions and get a better understand of multi-dimensional pollution interactions, especially between the upper layer and the surface.

This study is intended to use an online coupled chemical weather platform of Weather Research and Forecasting (WRF)/China Meteorological Administration Unified Atmospheric Chemistry Environment (CUACE) in order to analyze and evaluate the SO<sub>2</sub> in-cloud oxidation process in four polluted regions in China, with two objectives: (1) evaluating the cloud chemistry scheme in WRF/CUACE using in situ cloud chemistry observations at Mount Tai in the summers of 2015 and 2018 and (2) quantifying the contributions of cloud chemistry to the SO<sub>2</sub> and sulfate changes in a typical winter pollution month of December 2016 with a very long-lasting heavy pollution episode. It is aimed to establish a system to assess the relative contribution of cloud chemistry to SO<sub>2</sub> oxidation and sulfate productions vs. other clear-sky processes.

## 2 Model description and methodology

### 2.1 Cloud chemistry in WRF/CUACE

WRF/CUACE is an online coupled chemical weather model under the WRF framework with a comprehensive chemical module – CUACE, which is developed at CMA (China Meteorological Administration) with sectional aerosol physics, gas chemistry, aerosol–cloud interactions, and thermodynamic equilibrium (Zhou et al., 2012, 2016; Gong et al., 2003; Gong and Zhang, 2008; Zhang et al., 2021). It treats seven types of aerosols, i.e., black carbon (BC), organic car-

bon (OC), sulfate, nitrate, ammonium, soil dust, and sea salt, as well as more than 60 gaseous species. The system can simulate the concentrations of PM<sub>10</sub>, PM<sub>2.5</sub>, and O<sub>3</sub> as well as visibility. A complete heterogeneous chemistry module has been built in CUACE for nine gas-to-particle heterogeneous reactions including SO<sub>2</sub> to sulfate (C. Zhou et al., 2021; Zhang et al., 2021). The cloud chemistry mechanism in CUACE considers the pathways of multiphase oxidation of SO<sub>2</sub> by H<sub>2</sub>O<sub>2</sub> and O<sub>3</sub> in both stratocumulus and convective clouds (Gong et al., 2003; Von Salzen et al., 2000). The transport and chemical effects of sulfur in convective clouds are calculated based on a convective cloud model by WRF. Within the cloudy part of a grid box, the first-order rate constant (in s<sup>-1</sup>) of S(IV) (= SO<sub>2</sub>, HSO<sub>3</sub><sup>-</sup>, SO<sub>3</sub><sup>2-</sup>) oxidation is given by the following expression:

$$F = \left| \frac{1}{C_{S(IV)}} \frac{dC_{S(IV)}}{dt} \right| = F_1 C_{O_3} + F_2 C_{H_2O_2}, \quad (1)$$

where  $C_{S(IV)}$  is the total concentration of S(IV) (gas phase plus dissolved),  $C_{O_3}$  is the total concentration of O<sub>3</sub>, and  $C_{H_2O_2}$  is the total concentration of hydrogen peroxide.

The effective rate constants  $F_1$  and  $F_2$  are given by the following expressions:

$$F_1 = R_{O_3} f_1, \quad (2)$$

$$F_2 = R_{H_2O_2} f_2. \quad (3)$$

The reaction rate constants of  $R_{O_3}$  and  $R_{H_2O_2}$  refer to Maahs (1983) and Martin et al. (1984):

$$R_{O_3} = \left\{ 4.4 \times 10^{11} \exp(-4131/T) + 2.61 \times 10^3 \exp(-966/T) [H^+]^{-1} \right\} (\text{Ms})^{-1}, \quad (4)$$

$$R_{H_2O_2} = 8 \times 10^4 \exp[-3650(1/T - 1/298)] \{0.1 + [H^+]\}^{-1} (\text{Ms})^{-1}. \quad (5)$$

In Eqs. (2) and (3), the factors of  $f_1$  and  $f_2$  represent the partitioning of the substance between the aqueous and gas phases and are determined by the Henry's law coefficients.

$$f_1 = \gamma f_{SO_2} f_{O_3} K_S \bar{K}_{HO}, \quad (6)$$

$$f_2 = \gamma f_{SO_2} f_{H_2O_2} \bar{K}_{HS} \bar{K}_{HP}, \quad (7)$$

where  $\gamma$  is the dimensionless volume fraction of liquid water in the cloud. The parameters of  $f_{SO_2}$ ,  $f_{O_3}$ , and  $f_{H_2O_2}$  are the proportions of individual substances in the gas phase, which are calculated from the dimensionless Henry's law constant

and  $\gamma$ .

$$f_{SO_2} = (1 + \gamma \bar{K}_{HS} K_S)^{-1}, \quad (8)$$

$$f_{O_3} = (1 + \gamma \bar{K}_{HO})^{-1}, \quad (9)$$

$$f_{H_2O_2} = (1 + \gamma \bar{K}_{HP})^{-1}, \quad (10)$$

with

$$K_S = \bar{K}_{HS} \left( 1 + \frac{K_{1S}}{[H^+]} + \frac{K_{1S} K_{2S}}{[H^+]^2} \right). \quad (11)$$

The Henry's law constants used in Eqs. (6) to (8) are listed in Table 1.

In order to consider the dependence of the oxidation rates on pH, the H<sup>+</sup> concentration is calculated from the ion balance.

$$[H^+] + [NH_4^+] = [OH^-] + 2[SO_4^{2-}] + 2[SO_3^{2-}] + [HSO_3^-] + [NO_3^-] + [HCO_3^-] \quad (12)$$

From Eqs. (1)–(12), CUACE can simulate the oxidation rates of SO<sub>2</sub> by H<sub>2</sub>O<sub>2</sub> and O<sub>3</sub> mainly in the liquid and gaseous environment in both stratocumulus and convective clouds in a three-dimensional way.

## 2.2 Assessment criteria

Three variables, RTCLD, DT, and RT, are defined to assess the impact of cloud chemistry on SO<sub>2</sub> and sulfate. RTCLD refers to the concentration change ratio of substance  $i$  before and after the cloud chemical processes in a model run.

$$RTCLD(i) = 1 - \frac{BECLD(i)}{AFCLD(i)}, \quad (13)$$

where BECLD and AFCLD denote the concentrations of component  $i$  before and after the cloud chemical processes, respectively, and  $i$  denotes the chemical component of SO<sub>2</sub>, O<sub>3</sub>, H<sub>2</sub>O<sub>2</sub>, and sulfate.

DT indicates the difference in concentration of substance  $i$  with (CLD) and without ( $n$ CLD) the cloud chemistry module activated:

$$DT(i) = CLD(i) - nCLD(i), \quad (14)$$

and RT represents the concentration ratio change of the substance  $i$  with and without cloud chemistry in separate model runs:

$$RT(i) = 1 - \frac{nCLD(i)}{CLD(i)}. \quad (15)$$

## 2.3 Methodology

### 2.3.1 Model evaluation – Case 1

Mount Tai, located in central Shandong Province with an altitude of 1483 m, is the highest point of the NCP. It is an

**Table 1.** Equilibrium constants for the parameterization of the cloud chemistry in CUACE.

Equilibrium relation	Constant expression	Equilibrium constant		
		K (298)	a*	unit
$\text{SO}_2(\text{g}) + \text{H}_2\text{O}(\text{aq}) \leftrightarrow \text{SO}_2(\text{aq})$	$K_{\text{HS}} = \frac{[\text{SO}_2(\text{aq})]}{[\text{SO}_2(\text{g})]}$	1.23	3120	$\text{M atm}^{-1}$
$\text{SO}_2(\text{aq}) \leftrightarrow \text{H}^+ + \text{HSO}_3^-$	$K_{1\text{S}} = \frac{[\text{H}^+][\text{HSO}_3^-]}{[\text{SO}_2(\text{aq})]}$	$1.7 \times 10^{-2}$	2090	M
$\text{HSO}_3^- \leftrightarrow \text{H}^+ + \text{SO}_3^{2-}$	$K_{2\text{S}} = \frac{[\text{H}^+][\text{SO}_3^{2-}]}{[\text{HSO}_3^-]}$	$6.0 \times 10^{-8}$	1120	M
$\text{O}_3(\text{g}) + \text{H}_2\text{O}(\text{aq}) \leftrightarrow \text{O}_3(\text{aq})$	$K_{\text{HO}} = \frac{[\text{O}_3(\text{aq})]}{[\text{O}_3(\text{g})]}$	$1.15 \times 10^{-2}$	2560	$\text{M atm}^{-1}$
$\text{H}_2\text{O}_2(\text{g}) + \text{H}_2\text{O}(\text{aq}) \leftrightarrow \text{H}_2\text{O}_2(\text{aq})$	$K_{\text{HP}} = \frac{[\text{H}_2\text{O}_2(\text{aq})]}{[\text{H}_2\text{O}_2(\text{g})]}$	$9.7 \times 10^4$	6600	$\text{M atm}^{-1}$

\* “K (298)” and “a” are constants in  $K = k(298)[a(1/T - 1/298)]$ .

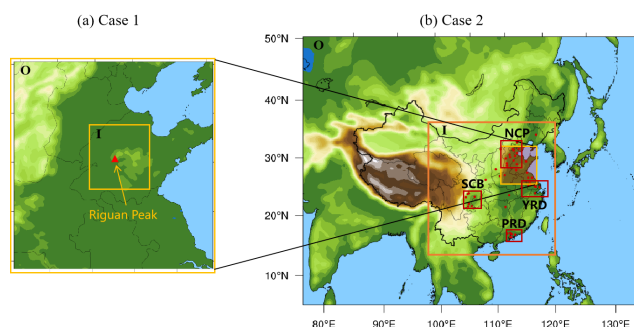


**Figure 1.** Model nesting domains and target regions. Case 1 (a): the red triangle is the Mount Tai observation site. Case 2 (b): red dots are cities where the surface observations of air pollutants are used for model evaluation. The target four regions are the NCP, YRD, PRD, and SCB.

ideal observation site for cloud chemistry observation (J. Li et al., 2017, 2020a, b). The observed concentrations of  $\text{SO}_2$ ,  $\text{O}_3$ ,  $\text{H}_2\text{O}_2$ , and sulfate in cloudy conditions from 19 June to 30 July 2015 and from 20 June to 30 July 2018 with a time interval of 1 h are obtained to evaluate the cloud chemistry scheme in WRF/CUACE (J. Li et al., 2017; Li et al., 2020a, b).

The WRF/CUACE is set up with two-level nesting domains for the evaluation with the Riguan Peak as the central point (Fig. 1a). The horizontal resolution of the outer domain (O) is 9 km with a grid of  $100 \times 104$ , and the horizontal resolution of the inner domain (I) is 3 km with a grid of  $88 \times 94$  (Fig. 1a). There are 32 vertical layers with a top pressure of 100 hPa.

### 2.3.2 Simulations of regional characteristics – Case 2

December 2016 was selected to assess the regional contribution of cloud chemistry to  $\text{SO}_2$  and sulfate in CUACE as a

**Table 2.** Physics parameterization schemes in WRF.

Physical management	Parameterization	References
Microphysics scheme	Lin	Lin et al. (1983)
Shortwave radiation	Goddard	Chou and Suarez (1994)
Longwave radiation	RRTM	Mlawer et al. (1997)
Land surface scheme	Noah	Chen and Dudhia (2001)
Boundary layer scheme	MYJ	Janjić (1994)
Cumulus scheme	Grell-3D	Grell (1993)

typical heavy pollution episode occurred from 16 to 22 December, covering most of east China, with the highest hourly  $\text{PM}_{2.5}$  concentration exceeding  $1100 \mu\text{g m}^{-3}$ . The simulation region is set up as shown in Fig. 1b with two-level nesting domains. The outer domain covers Central and East Asia with a horizontal resolution of 54 km and a grid of  $139 \times 112$ . The inner domain covers most of China on the eastern side of the Qinghai–Tibet Plateau including NCP, YRD, PRD, and SCB, with a horizontal resolution of 18 km and a grid of  $157 \times 166$ . The vertical layer number of the model is the same as that in Case 1.

Since the cloud water is the reaction pool of cloud chemistry, whether the simulation of cloud water is reasonable or not is directly related to the effectiveness of cloud chemistry. Both the cloud water and rainwater from WRF are online coupled to the cloud chemistry module, and the main physics configurations are listed in Table 2.

### 2.4 Meteorological, pollution, and satellite data

For both cases, the meteorological initial and boundary conditions for WRF/CUACE are from the National Centers for Environmental Prediction (NCEP) FNL (Final) global re-analysis at a resolution of  $1^\circ \times 1^\circ$  with 6 h interval. The chemical lateral boundary conditions are from the National

Oceanic and Atmospheric Administration (NOAA) Meteorological Laboratory Regional Oxidant Model (NALROM; Liu et al., 1996). The model is run in a restart way with a 5 d spin-up.

FY-2G cloud image data from CMA with a 1 h interval are used to evaluate the cloud in both cases. Routine meteorological observations at a 3 h interval from 23 meteorological stations of CMA for 2 m temperature, 2 m relative humidity, and 10 m wind speed as well as hourly pollutant data for 55 city sites from the China National Environmental Monitoring Centre are used to evaluate the meteorological fields and pollutants for December 2016. For a city with several observation sites, an averaged value is used.

MEIC (Multi-resolution Emission Inventory for China), at a resolution of  $0.25^\circ$ , is used as the anthropogenic emissions with species of  $\text{SO}_2$ , nitrogen oxides ( $\text{NO}_x$ ), carbon monoxide (CO), ammonia ( $\text{NH}_3$ ), BC, OC, non-methane volatile organic compounds (NMVOCs),  $\text{PM}_{2.5}$ , and  $\text{PM}_{10}$  from industry, transportation, residential areas, and agriculture (M. Li et al., 2017; Zheng et al., 2018). The emission base years of 2015 and 2017 are used for Case 1 and Case 2, respectively.

### 3 Results and discussion

#### 3.1 Evaluation of the cloud chemistry mechanism

In order to evaluate the cloud chemistry mechanism in WRF/CUACE, the simulation results are compared with the observations at Mount Tai. By analyzing the satellite cloud images in and around Mount Tai and matching with the available observed data, two time periods with clouds, from 19 June to 30 July 2015 and from 20 June to 30 July 2018, were selected for the comparisons, defined as “cloud process-1” (CP-1) and “cloud process-2” (CP-2), respectively. The simulated results for chemical species are illustrated in scatterplots (Fig. 2), which reveals that the simulated concentrations of  $\text{SO}_2$ , sulfate,  $\text{O}_3$ , and  $\text{H}_2\text{O}_2$  are all within a factor of 2 of the observations when cloud chemistry occurs, indicating reasonable agreement between simulations and observations for both CP-1 and CP-2 cases. The sulfate underestimates are clear in both CP-1 and CP-2 cases, which was reported by other modeling results as well (Tuccella et al., 2012; Huang et al., 2019; Ge et al., 2022).

The statistics of correlation coefficients ( $R$ ), relative average deviation (RAD), and normalized mean deviation (NMB) between hourly simulated and observed  $\text{SO}_2$ ,  $\text{O}_3$ ,  $\text{H}_2\text{O}_2$ , and sulfate are shown in Table 3. Among them, the simulated and observed averages of  $\text{SO}_2$  are very close in both CP-1 and CP-2, with a RAD about  $-3.4\%$  and  $-6.1\%$ . For other species, the RAD is in the range of  $8.7\%$ – $55.0\%$ . The  $R$  values for the four species are 0.34, 0.33, 0.78, and 0.32 for CP-1 and 0.47, 0.40, 0.06, and 0.54 for CP-2, respectively. Although the  $R$ , RAD, and NMB of  $\text{H}_2\text{O}_2$  in CP-2 are only 0.06,  $18.0\%$ , and  $-19.6\%$ , the simulated mean value of  $\text{H}_2\text{O}_2$  is closer to the observed mean value than

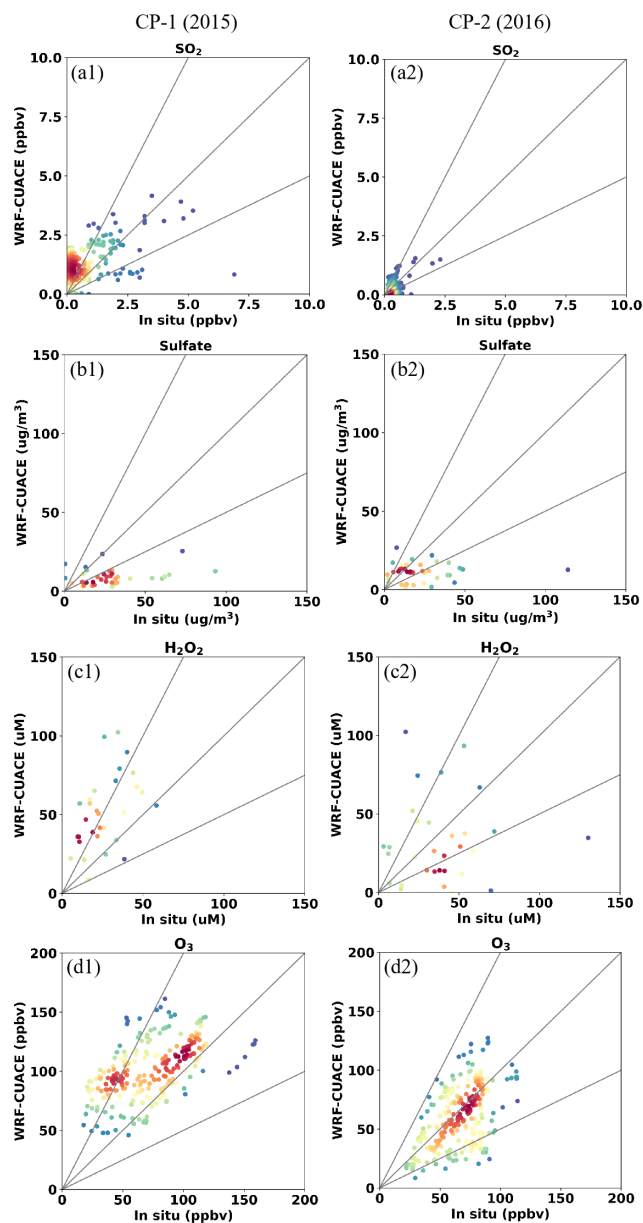


**Figure 2.** Scatterplots of hourly  $\text{SO}_2$  (a1, a2), sulfate (b1, b2),  $\text{H}_2\text{O}_2$  (c1, c2), and  $\text{O}_3$  (d1, d2) concentrations between WRF/CUACE and in situ observations at Mount Tai in CP-1 and CP-2. Units:  $\text{SO}_2$  and  $\text{O}_3$  (ppbv),  $\text{H}_2\text{O}_2$  ( $\mu\text{M}$ ), and sulfate ( $\mu\text{g m}^{-3}$ ). The color of the dots represents the point density, and the red means larger sample size.

that of CP-1 (RAD =  $22.4\%$ , NMB =  $-36.6\%$ ). For sulfate, the simulated  $R$  values are 0.32 and 0.54 in CP-1 and CP-2, respectively, but the model underestimates sulfate concentrations with NMB of  $-71.0\%$  and  $-59.4\%$  in CP-1 and CP-2. Some reasons might contribute to the underestimations. Firstly, the latitude of the observed site at Mount Tai is  $1483\text{ m}$ , which can be in the boundary layer during the daytime and in the free atmosphere during the nighttime

in summer (Zhu et al., 2018). Therefore, the diurnal variation of the boundary layer affects the three-dimensional concentration distribution of oxidants and aerosols (Peng et al., 2021) and influences the development of cloud formation. Secondly, there are biases from the model due to the difficulties of representing the complex topography of Mount Tai and cloud physics. Thirdly, the cloud chemistry in CUACE lacks a pathway for TMI- and  $\text{NO}_2$ -catalyzed oxidation, as well as some other newly discovered oxidation mechanisms, which could lead to the bias in  $\text{SO}_2$  and sulfate. Fourthly, typical measurement systems for ambient aerosols easily misinterpret organosulfur (mainly in the presence of hydroxymethane sulfonate, HMS) as inorganic sulfate, thus leading to a positive observational bias, e.g., 20 % mean bias during winter haze in Beijing (Moch et al., 2018; Song et al., 2019).

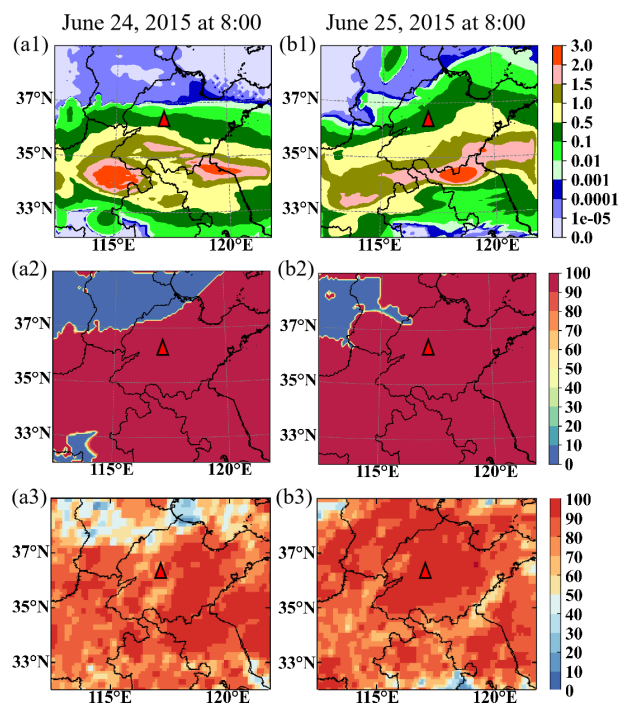
Another interesting point simulated correctly by the model was the increasing trend of  $\text{H}_2\text{O}_2$  and the decreasing trend of  $\text{SO}_2$  from 2015 to 2018. The observed and simulated mean values of  $\text{H}_2\text{O}_2$  were changed from 26.5 and 16.8  $\mu\text{M}$  in CP-1 in 2015 to 46.9 and 32.4  $\mu\text{M}$  in CP-2 in 2018, respectively. For  $\text{SO}_2$ , the observed and simulated mean values were reduced from 2.2 and 2.3  $\mu\text{g m}^{-3}$  in CP-1 in 2015 to 0.6 and 0.6  $\mu\text{g m}^{-3}$  in CP-2 in 2018, respectively (Table 3). Both the observations and simulations clearly showed the increasing trend of  $\text{H}_2\text{O}_2$  and the decreasing trend of  $\text{SO}_2$  from 2015 to 2018. This conclusion is consistent with the trends of other observational studies (Ren et al., 2009; Shen et al., 2012; Li et al., 2020a; Ye et al., 2021). The decreasing  $\text{SO}_2$  and increasing  $\text{H}_2\text{O}_2$  and  $\text{O}_3$  have been attributed to the national  $\text{SO}_2$  and particulate emission control measures since 2013 (Fan et al., 2010; Lu et al., 2020).

Figure 4 shows the RTCLD of  $\text{SO}_2$  and simulated liquid water content at 02:00 and 08:00 LST on both 24 and 25 June in CP-1 at Mount Tai. The column cloud and the liquid water content, which are consistent with the cloud images, indicate that there are clouds with sufficient water vapor in and around the vicinity of Mount Tai (Fig. 3). The  $\text{SO}_2$  consumption rate (RTCLD( $\text{SO}_2$ )) distribution is consistent with the liquid water distribution at all four times (Fig. 4). The  $\text{SO}_2$  depletion rate is above 80 % at Mount Tai, which is compatible with observations (Li, 2020). All of these indicate that the model can capture the  $\text{SO}_2$  consumption in the cloudy environment.

In summary, the simulated  $\text{SO}_2$ ,  $\text{H}_2\text{O}_2$ ,  $\text{O}_3$ , and sulfate concentrations are comparable to the observations. WRF/CUACE is also able to simulate the decreasing trend of  $\text{SO}_2$  and the increasing trends of  $\text{O}_3$  and  $\text{H}_2\text{O}_2$  over the year. Therefore, the cloud chemistry mechanism in WRF/CUACE is relatively reasonable for reproducing the cloud chemistry for  $\text{SO}_2$ , sulfate, and the important oxidants of  $\text{H}_2\text{O}_2$  and  $\text{O}_3$ .

### 3.2 Assessment of the impacts of cloud chemistry on regional $\text{SO}_2$ and sulfate

This section will further assess the contribution of cloud chemistry for the four main pollution regions of NCP, YRD,



**Figure 3.** Cloud water simulation and satellite comparison. The column liquid water content by WRF/CUACE (a1, b1, unit:  $\text{kg m}^{-2}$ ), the cloud fraction by WRF/CUACE (a2, b2, unit: %), and the cloud total amount of FY2G, (a3, b3, unit: %). Panel (a) is for 08:00 LST on 24 June 2015, and (b) is for 08:00 LST on 25 June 2015. The red triangle is the Mount Tai observation site.

PRD, and SCB (Fig. 1b) in China for all of December of 2016 (hereinafter referred to as DEC) and a heavy pollution episode (hereinafter referred to as HPE) occurring during the month (16–22 December), as selected for Case 2. The regional impacts of cloud chemical processes on surface  $\text{SO}_2$  and sulfate are analyzed for DEC and for HPE. The heavy pollution episode (HPE) is investigated with respect to the developing stage HPE-1 (16–18 December 2016), the maturity stage HPE-2 (19–21 December 2016), and the dissipation stage HPE-3 (22 December 2016) for the four pollution regions.

#### 3.2.1 Meteorological evaluation

As the driving force for air pollution and cloud chemistry, the meteorology elements of 2 m temperature (T2), 2 m relative humidity (RH2), and 10 m wind speed (WS10) in DEC and HPE are compared between simulated and observed results in Table 4. The temperature correlation is the best in DEC, followed by humidity and then wind speed, which is consistent with previous findings (Zhou et al., 2012; Wang et al., 2015; Gao et al., 2016). The RMSEs of wind speeds all range from 1.03 to 1.50  $\text{m s}^{-1}$ , falling within the criteria (less than 2  $\text{m s}^{-1}$ ) defining “good” model performance in stagnant weather (Emery et al., 2001). The RMSE of wind

**Table 3.** Statistics for SO<sub>2</sub>, O<sub>3</sub>, H<sub>2</sub>O<sub>2</sub>, and sulfate in cloud chemistry at the Mount Tai site.

		Observed mean	Simulated mean	<i>R</i>	RAD (%)	NMB (%)
CP-1	SO <sub>2</sub>	2.2	2.3	0.34	−3.4	7.1
	O <sub>3</sub>	97.8	55.3	0.33	27.8	−43.5
	H <sub>2</sub> O <sub>2</sub>	26.5	16.8	0.78	22.4	−36.6
	Sulfate	31.7	9.2	0.32	55.0	−71.0
CP-2	SO <sub>2</sub>	0.6	0.6	0.47	−6.1	12.9
	O <sub>3</sub>	60.7	51.0	0.40	8.7	−16.0
	H <sub>2</sub> O <sub>2</sub>	46.9	32.4	0.06	18.4	−29.6
	Sulfate	28.1	11.4	0.54	42.2	−59.4

Units: SO<sub>2</sub> and O<sub>3</sub> (ppbv), H<sub>2</sub>O<sub>2</sub> (μM), and sulfate (μg m<sup>−3</sup>).

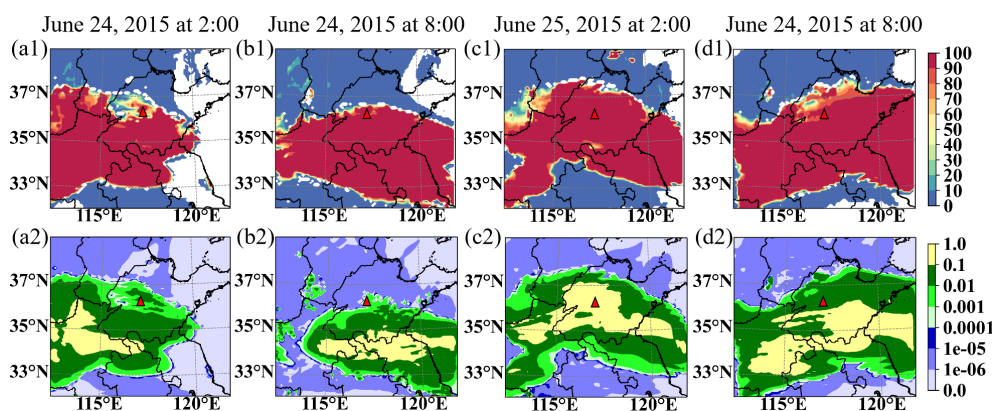


**Figure 4.** Regional comparison of in-cloud SO<sub>2</sub> oxidation with cloud water at the top of Mount Tai. Distributions of SO<sub>2</sub> oxidation rate (a1, b1, c1, and d1, unit: %) and liquid water content (a2, b2, c2, and d2, unit: g kg<sup>−1</sup>) by WRF/CUACE, where (a) is for 02:00 LST on 24 June 2015, (b) is for 08:00 LST on 24 June 2015, (c) is for 02:00 LST on 25 June 2015, and (d) is for 08:00 LST on 25 June 2015. The red triangle is the Mount Tai observation site.

speed and the wind speed for HPE is smaller than that of DEC, which indicates that the model can relatively reasonably capture the static condition.

Figure 5 shows the satellite cloud images, the column cloud, and the liquid water content simulated for the maturity and dissipation stages (19–22 December) of the HPE. The satellite image shows that the cloud coverage region is mainly in the southwest of China, besides SCB on 19 December, covering most of eastern China including NCP, YRD, PRD, and SCB on December 20 and 21, and then moving eastward outside of China on December 22 (Fig. 5a1–d1). The cloud distribution fits well with the satellite images (Fig. 5a2–d2). The column liquid water distribution also moves from west to east as the episode developed (Fig. 5a3–d3), which is located farther south in eastern China than that of the clouds. In SCB and YRD, the liquid water content is more abundant, reaching over 100.0 g m<sup>−2</sup>, than that in PRD, only up to 10.0 g m<sup>−2</sup>. NCP has the least liquid water content among the four regions, especially in Beijing and the northwestern part of Hebei Province ranging over 0.001–0.01 g m<sup>−2</sup>, mostly due to the dry environment and partly

due to the overestimated temperature and underestimated humidity in the model. Above all, CUACE not only effectively simulates pollution but also provides a relatively reasonable meteorological background basis for cloud chemistry in the heavy pollution period.

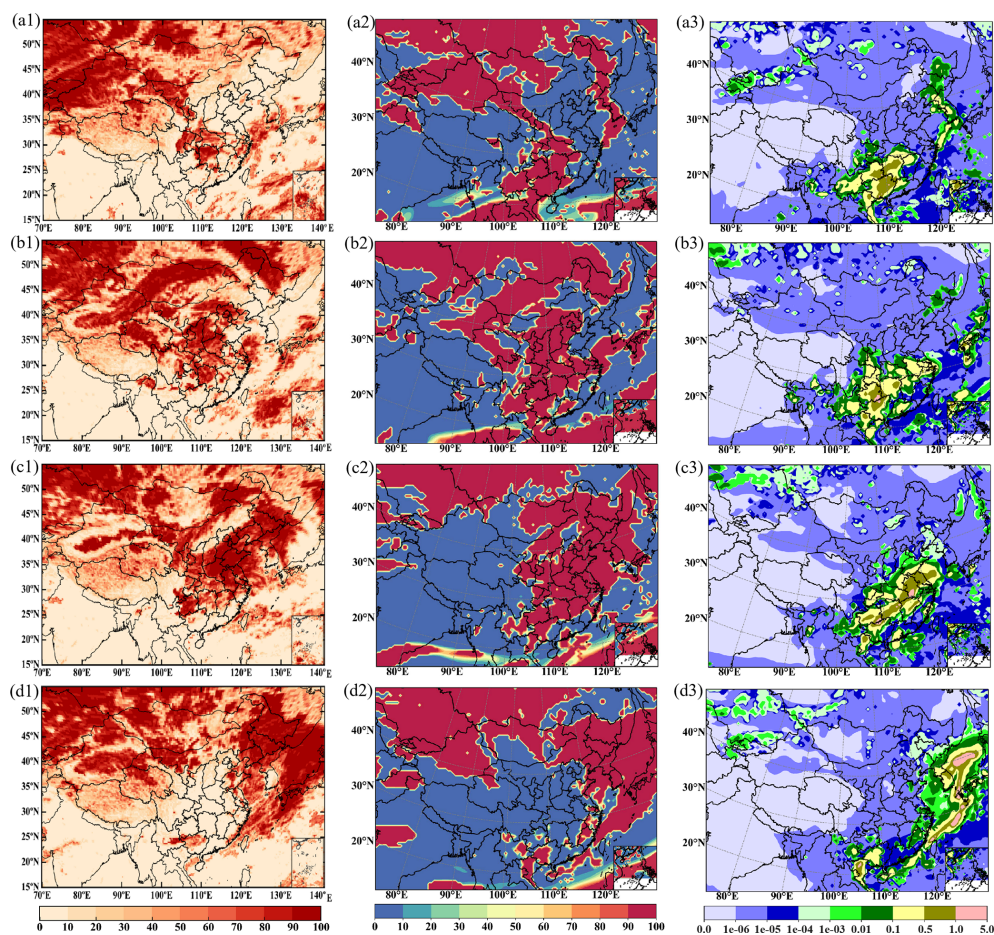
### 3.2.2 Chemical evaluation

Figure 6 shows the mean SO<sub>2</sub> and sulfate concentrations simulated for DEC and HPE-2. The high and low centers of monthly mean SO<sub>2</sub> and sulfate concentrations by CUACE in December 2016 coincided with the annual observed average by Cao et al. (2021) in the SCB and NCP. The sulfate concentrations are low on a monthly basis and high at the pollution maturity stage compared to the averaged observations of several pollution episodes studied by Wang et al. (2022) in December 2016 for NCP. The simulated mean sulfate concentration distribution in Fig. 6b is comparable to that by Wang et al. (2021, 2022) in December 2016, both displaying an increase from northwest to southeast almost of the same magnitude as in NCP. For SCB, sulfate concentrations

**Table 4.** Statistical metrics for meteorology in four regions for HPE and DEC.

		Observed mean		Simulated mean		<i>R</i>		NMB (%)		RMSE	
		HPE	DEC	HPE	DEC	HPE	DEC	HPE	DEC	HPE	DEC
NCP	T2	1.0	1.1	2.8	2.1	0.70	0.84	187.3	84.9	3.3	2.5
	RH2	78.8	68.3	52.3	48.8	0.54	0.64	−33.7	−28.6	32.3	25.9
	WS10	1.5	1.7	1.7	2.2	0.49	0.54	14.1	27.5	1.2	1.3
YRD	T2	9.2	8.0	9.5	8.4	0.94	0.96	2.9	5.1	1.4	1.3
	RH2	79.2	75.6	73.8	73.0	0.86	0.85	−6.8	−3.5	10.7	9.3
	WS10	2.2	2.3	2.8	3.0	0.74	0.76	28.7	31.9	1.2	1.3
PRD	T2	18.3	17.3	19.0	17.9	0.93	0.92	3.6	3.8	1.9	1.9
	RH2	72.2	70.4	64.3	65.4	0.76	0.68	−10.9	−7.2	14.0	13.9
	WS10	1.8	2.4	2.0	3.2	0.67	0.72	13.6	37.1	1.0	1.5
SCB	T2	10.2	9.7	10.5	10.0	0.74	0.75	2.8	3.1	1.8	2.2
	RH2	81.6	79.9	74.1	71.3	0.66	0.60	−9.2	−10.8	12.7	15.5
	WS10	1.1	1.3	1.6	1.9	0.49	0.36	49.2	50.5	1.0	1.3

Units: T2 (°), RH2 (%), and WS10 (m s<sup>−1</sup>).



**Figure 5.** Cloud water simulation and satellite comparison in a heavy pollution episode. The cloud total amount of FY-2G (a1, b1, c1, d1, unit: %), the column cloud of WRF/CUACE (a2, b2, c2, d2, unit: %), and the column liquid water content of WRF/CUACE (a3, b3, c3, d3, unit: kg m<sup>−2</sup>). Panel (a) is for 08:00 LST on 19 December, (b) is for 08:00 LST on 20 December, (c) is for 08:00 LST on 21 December, and (d) is for 08:00 LST on 22 December.

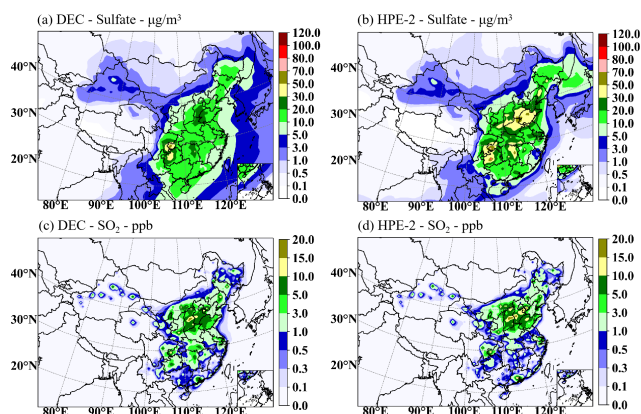


**Figure 6.** The mean sulfate concentration for DEC (a, c) and HPE-2 (b, d) for SO<sub>2</sub> (c, d) and sulfate (a, b).

are compatible to that observed in winter in 2015 by Kong et al. (2020).

The simulated hourly PM<sub>2.5</sub>, O<sub>3</sub>, and SO<sub>2</sub> concentrations in four regions are also compared with the observations (Table 5). Most of the simulations are within a factor of 2 of the observations (figure omitted), and the mean values of the three pollutants in the four regions are close to the observations for DEC and HPE, indicating that the model captures the variability of PM<sub>2.5</sub>, O<sub>3</sub>, and SO<sub>2</sub> concentrations for both DEC and HPE. During HPE, the differences of mean values ranged from  $-7.6$  to  $10.4 \mu\text{g m}^{-3}$  for SO<sub>2</sub>, from  $-22$  to  $23.3 \mu\text{g m}^{-3}$  for O<sub>3</sub>, and from  $-156.5$  to  $48.8 \mu\text{g m}^{-3}$  for PM<sub>2.5</sub>. During DEC, the differences of mean values were from  $-21.5$  to  $-1.2 \mu\text{g m}^{-3}$  for SO<sub>2</sub>, from  $1.1$  to  $7.7 \mu\text{g m}^{-3}$  for O<sub>3</sub>, and from  $-71.3$  to  $1.3 \mu\text{g m}^{-3}$  for PM<sub>2.5</sub>. During HPE, the *R* values are from 0.32 to 0.61 for SO<sub>2</sub>, from 0.20 to 0.84 for O<sub>3</sub>, and from 0.27 to 0.84 for PM<sub>2.5</sub>. During DEC, the *R* values are from 0.19 to 0.48 for SO<sub>2</sub>, from 0.47 to 0.80 for O<sub>3</sub>, and from 0.28 to 0.73 for PM<sub>2.5</sub>. During HPE, the NMBs are from  $-49.8$  to  $46.3$  for SO<sub>2</sub>, from  $-54.0$  to  $123.1$  for O<sub>3</sub>, and from  $-48.2$  to  $51.0$  for PM<sub>2.5</sub>. During DEC, the NMBs are from  $-47.4$  to  $11.9$  for SO<sub>2</sub>, from  $-45.5$  to  $97.4$  for O<sub>3</sub>, and from  $-35.7$  to  $51.5$  for PM<sub>2.5</sub>. The simulation in PRD, YRD, and NCP is relatively better than that in the SCB, where the complex terrain poses great challenges to meteorological field simulations.

The ability of CUACE to simulate SO<sub>2</sub>, O<sub>3</sub>, and sulfate concentrations has also been evaluated in many previous research applications (Ke et al., 2020; Y. Zhou et al., 2021; Zhang et al., 2021). Ke et al. (2020) reported that the correlation between CUACE modeled and observed PM<sub>2.5</sub> was 0.41–0.85 in NCP and 0.64–0.74 in YRD. Other atmospheric models in China have shown the same performance: for example, NACRMS has a correlation of about 0.68 for PM<sub>2.5</sub> in NCP during a haze period (Wang et al., 2014).

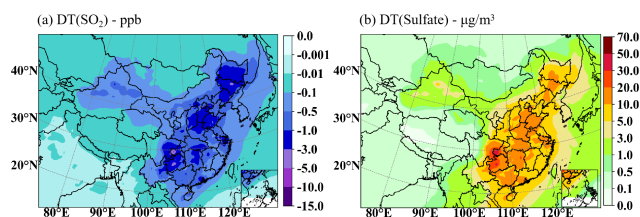


**Figure 7.** The mean SO<sub>2</sub> concentration decreased (a) and sulfate concentration increased (b) by cloud chemistry for DEC.

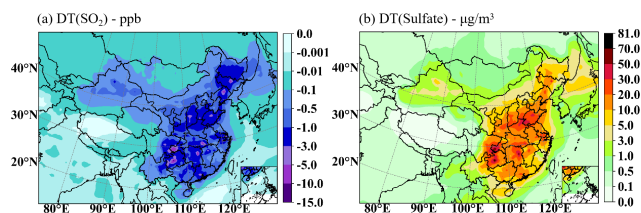
### 3.2.3 Assessment of regional contributions

In order to assess the regional contributions, the average monthly impact of cloud chemistry on surface SO<sub>2</sub> and sulfate denoted by DT (SO<sub>2</sub>) and DT (sulfate) for DEC is investigated (Fig. 7). It is found that the SO<sub>2</sub> reduction for DEC is concentrated mostly in the central-east part of China, by an average of 0.1–1.0 ppb in most regions by cloud chemistry. SO<sub>2</sub> concentrations are reduced by 0.5–3.0 ppb in most of the NCP, YRD, PRD, and SCB regions. Among them, there is a relatively strong center decreasing by 3.0–10.0 ppb in SCB. Ge et al. (2021) have evaluated the effects of in-cloud aqueous-phase chemistry on SO<sub>2</sub> oxidation in the Community Earth System Model version 2 (CESM2). They found that the results incorporating detailed cloud aqueous-phase chemistry greatly reduced the SO<sub>2</sub> overestimation, i.e., by 0.1–10.0 ppb in China and more than 10.0 ppb in some regions in winter, which is consistent with the results demonstrated in Fig. 7, where SO<sub>2</sub> concentrations are depleted by 0.1–10 ppb in China. Correspondingly, sulfate growth is mainly centered in SCB, with the increased maximum up to  $20.0$ – $50.0 \mu\text{g m}^{-3}$ . Sulfate concentrations are increased by  $10.0$ – $20.0 \mu\text{g m}^{-3}$  in most parts of NCP, YRD, and PRD and by  $5$ – $10.0 \mu\text{g m}^{-3}$  in others.

In addition to the average monthly impact of cloud chemistry, Fig. 8 shows DT(SO<sub>2</sub>) and DT(sulfate) for HPE-2. It is found that the SO<sub>2</sub> concentration decreases most significantly in SCB: by 1.0–3.0 ppb in most regions and up to 3.0–10.0 ppb in the central region. In YRD, PRD, and NCP, the reduction reaches 1.0–3.0 ppb in most parts, while the smallest decrease is below 1.0 ppb in the northern part of NCP. Meanwhile, in terms of regional distribution, the regions of increasing sulfate and decreasing SO<sub>2</sub> concentrations are correlated, but not identical. Sulfate production is mainly focused in SCB, with the increasing maximum up to  $20.0$ – $50.0 \mu\text{g m}^{-3}$ , while production is  $10.0$ – $20.0 \mu\text{g m}^{-3}$  in most parts of NCP, YRD, and PRD and  $5.0$ – $10.0 \mu\text{g m}^{-3}$  in other regions. In Figs. 7b and 8b, the increasing rates for monthly mean sulfate concentrations are about 60 % to 70 % in NCP. The heaviest and longest duration pollution episode that had many clouds and high liquid water content (Fig. 5) on 19–21 December 2016 was very favorable for the occurrence of in-cloud oxidation processes. Sulfate formation rates by H<sub>2</sub>O<sub>2</sub> oxidation under winter haze conditions range from

**Table 5.** Statistical metrics for hourly SO<sub>2</sub>, O<sub>3</sub>, and PM<sub>2.5</sub> in four regions for HPE and DEC.

		Observed mean ( $\mu\text{g m}^{-3}$ )		Simulated mean ( $\mu\text{g m}^{-3}$ )		<i>R</i>		NMB (%)	
		HPE	DEC	HPE	DEC	HPE	DEC	HPE	DEC
NCP	SO <sub>2</sub>	42.0	61.5	50.0	40.0	0.60	0.48	46.3	-15.6
	O <sub>3</sub>	8.8	7.4	7.4	10.9	0.47	0.60	-15.3	-32.4
	PM <sub>2.5</sub>	351.3	182.1	194.8	110.8	0.30	0.62	-48.2	-35.7
YRD	SO <sub>2</sub>	21.8	16.3	15.8	14.9	0.61	0.45	-25.3	-32.8
	O <sub>3</sub>	31.3	14.4	9.3	22.1	0.33	0.68	-54.0	-45.5
	PM <sub>2.5</sub>	70.3	82.9	119.1	84.2	0.70	0.73	18.0	19.3
PRD	SO <sub>2</sub>	13.6	24.0	24.0	17.0	0.32	0.39	76.1	11.9
	O <sub>3</sub>	45.7	56.3	56.5	57.4	0.84	0.80	23.0	13.9
	PM <sub>2.5</sub>	55.7	83.6	83.8	77.5	0.84	0.39	50.1	51.5
SCB	SO <sub>2</sub>	20.0	10.0	12.4	8.8	0.49	0.19	-49.8	-47.4
	O <sub>3</sub>	22.0	49.0	45.3	54.2	0.20	0.47	123.1	97.4
	PM <sub>2.5</sub>	135.6	91.0	117.0	71.0	0.27	0.28	-32.9	-29.1

**Figure 8.** The mean SO<sub>2</sub> concentration decreased (a) and sulfate concentration increased (b) by cloud chemistry for HPE-2.

10 to 1000  $\mu\text{g m}^{-3} \text{ s}^{-1}$ , which is close to the range of 10 to 100  $\mu\text{g m}^{-3} \text{ s}^{-1}$  obtained by Wang et al. (2022) in several pollution episodes in December 2016, indicating that the in-cloud oxidation in this study is relatively reasonable.

Exploring details of the HPE, four time periods, 14:00 and 21:00 on December 20, 17:00 on December 21 of the HPE-2, and 12:00 on December 22 of the HPE-3, are used to specifically analyze the contribution of cloud chemistry. It is found that the cloud chemistry influence is mainly on SCB and YRD at 14:00 and 21:00 LST on 20 December for HPE-2. The observed PM<sub>2.5</sub> concentrations are very high, up to 350  $\mu\text{g m}^{-3}$  at 14:00 and 236  $\mu\text{g m}^{-3}$  at 21:00 on December 20 in Chengdu of SCB, and up to 76  $\mu\text{g m}^{-3}$  at 14:00 and 77  $\mu\text{g m}^{-3}$  at 21:00 on December 20 in Hangzhou of YRD, partially supporting the cloud production of sulfate at these specific times. Correspondingly, Fig. 9 shows that sulfate increases by cloud chemistry during these time periods are 10–20  $\mu\text{g m}^{-3}$  and 20–30  $\mu\text{g m}^{-3}$  14:00 and 21:00 on December 20 at Chengdu, and 20–60  $\mu\text{g m}^{-3}$  and 30–60  $\mu\text{g m}^{-3}$  at Hangzhou.

Above all, the contribution of cloud chemistry to surface sulfate during the HPE is the highest in the SCB, followed by the NCP, YRD, and PRD, with most concentration in-

creases ranging over 20.0–100.0  $\mu\text{g m}^{-3}$ , 10.0–60.0  $\mu\text{g m}^{-3}$ , 10.0–40.0  $\mu\text{g m}^{-3}$ , and 10.0–40.0  $\mu\text{g m}^{-3}$ , respectively, and less than 10.0  $\mu\text{g m}^{-3}$  in Beijing, Tianjin, and the northwestern part of Hebei Province (Fig. 9). Of particular note is the NCP region, where the contribution of cloud chemistry is not significant on a monthly average but is very significant and exceeds that for the YRD region at certain moments during HPE. This also provides an explanation for the explosive increase in particulate matter concentrations during HPE in this region.

Further analysis of the simulation characteristics with and without cloud chemistry on all the regions during the HPE-2 stage (Fig. 10) and the DEC (Fig. 11) is carried out. Compared with *n*CLD, *R* of SO<sub>2</sub> in CLD increases by 0.06, 0.15, and 0.01 in YRD, SCB, and NCP, respectively, and the overestimation in NCP and PRD has been corrected during HPE-2. *R* also increases by 0.10, 0.03, and 0.05 in YRD, SCB, and NCP for the DEC, respectively. It is obvious that the model simulates SO<sub>2</sub> concentrations better at NCP during HPE-2 than for DEC with cloud chemistry.

For PM<sub>2.5</sub>, the statistical results of the simulated mean, *R*, and NMB in CLD and *n*CLD in the four polluted regions do not differ significantly between HPE-2 and DEC, but there is a significant improvement in the underestimate of sulfate in NCP and SCB. Under cloud chemistry, the deviation in the NCP is reduced from -45.7% to -35.7% for DEC and from -52.6% to -48.2% for HPE-2. The deviation in SCB is also improved from -44.2% to -29.1% for DEC and from -46.5% to -32.9% for HPE-2. A significant reduction in the model's PM<sub>2.5</sub> concentration simulation bias after considering cloud chemistry and an improvement in the underestimate at NCP and SCB have been achieved.

Moreover, the statistical results of all stations (SUM in Fig. 12) show that after considering cloud chemical simu-

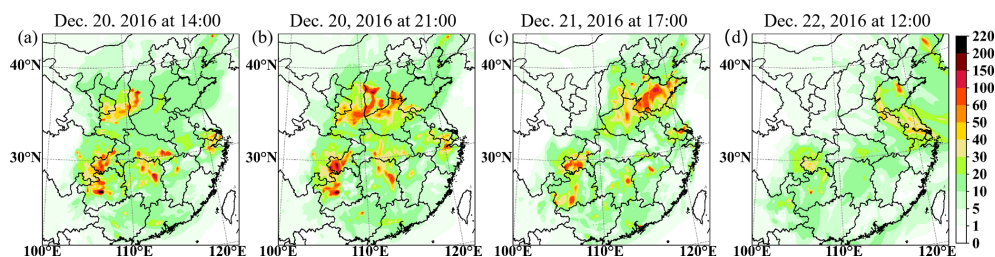


**Figure 9.** The differences in surface sulfate concentrations between with and without cloud chemistry at 14:00 (a) and 21:00 (b) LST on 20 December, at 17:00 LST on 21 December (c), and at 12:00 LST on 22 December (d, units:  $\mu\text{g m}^{-3}$ ).

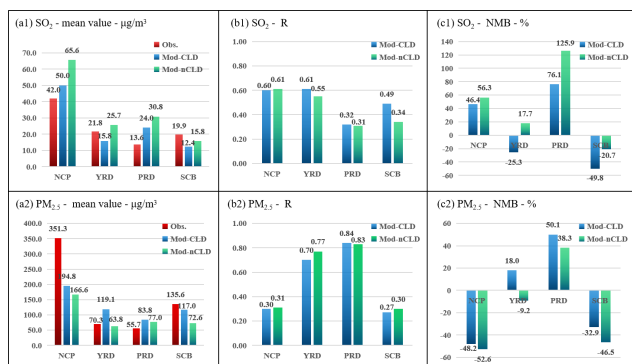


**Figure 10.** Statistical metrics for hourly SO<sub>2</sub> and PM<sub>2.5</sub> for four regions for HPE-2 with (Mod-CLD) and without (Mod-*n*CLD) cloud chemistry. The mean value (a1, unit:  $\mu\text{g m}^{-3}$ ), *R* (b1), and NMB (c1, unit: %) of SO<sub>2</sub>, as well as the mean value (a2, unit:  $\mu\text{g m}^{-3}$ ), *R* (b2), and NMB (c2, unit: %) of PM<sub>2.5</sub>. Obs. denotes the observations.

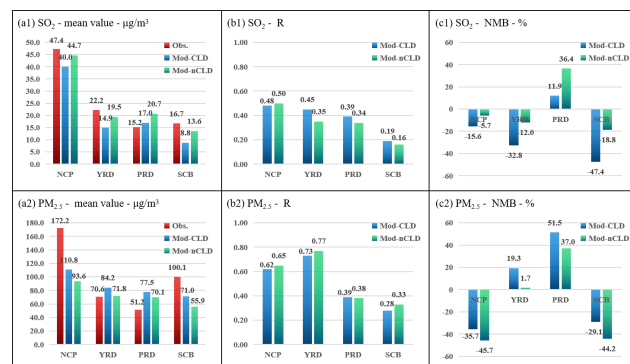


**Figure 11.** Statistical metrics for hourly SO<sub>2</sub> and PM<sub>2.5</sub> for four regions for DEC with (Mod-CLD) and without (Mod-*n*CLD) cloud chemistry. The mean value (a1, unit:  $\mu\text{g m}^{-3}$ ), *R* (b1), and NMB (c1, unit: %) of SO<sub>2</sub>, as well as the mean value (a2, unit:  $\mu\text{g m}^{-3}$ ), *R* (b2), and NMB (c2, unit: %) of PM<sub>2.5</sub>. Obs. denotes the observations.

lation (CLD), the NMB of SO<sub>2</sub> is decreased from 39.3 % to 13.8 % and the NMB of PM<sub>2.5</sub> from -40.8 % to -31.6 % during the HPE-2 after the addition of cloud chemistry simulation, reducing the simulation bias of both SO<sub>2</sub> and PM<sub>2.5</sub>. This indicates that the addition of cloud chemistry to the model improves the model for SO<sub>2</sub> and sulfate simulations. The improvement of sulfate simulation in the presence of clouds also contributes to the improvement of the simulation accuracy of PM<sub>2.5</sub> mentioned above.

In summary, comparing the contribution of cloud chemistry in DEC with HPE-2, it is found that the cloud chemistry in heavy pollution weather for SO<sub>2</sub> depletion and sulfate increase is mainly concentrated in central-east China and obviously in the four major pollution regions. However, SO<sub>2</sub> consumption and sulfate increase are not consistent, which is influenced not only by the local SO<sub>2</sub> concentration, but also by the cloud amount. Therefore, for SCB, which is less polluted and has many more clouds than NCP, the impact of cloud chemistry on sulfate and its precursor SO<sub>2</sub> is always the most significant for both HPE and DEC.

### 3.3 Site evaluation of cloud chemistry

The statistical metrics of SO<sub>2</sub> and PM<sub>2.5</sub> hourly concentrations in 55 representative cities with and without cloud chemistry in the model were analyzed. The results indicate that most of the sites are improved with cloud chemistry in the SO<sub>2</sub> concentration simulation and 42 of the 55 cities are with the increasing *R*. In the PM<sub>2.5</sub> simulation, the correlations also are improved in some cities after the presence of cloud chemistry.

Representative sites of Beijing, Nanjing, Guangzhou, and Chengdu in NCP, YRD, PRD, and SCB are selected to quantify the impact of cloud chemistry during the HPE. The net depletion ratio of SO<sub>2</sub> column concentration (RT(SO<sub>2</sub>)) during cloud chemistry is shown in Fig. 13. It is found that SO<sub>2</sub> column concentration reduction maintained mostly a high value of over 60 %, even 80 % sometimes, in Chengdu during HPE-2. In Nanjing, the SO<sub>2</sub> level was reduced by about 20 %–50 % from December 17 to 19 and by up to 80 % from December 20 to 21, when the episode matured there. The changes of SO<sub>2</sub> in these two cities are consistent with the changes in cloud and liquid cloud water content distributions during the HPE-2 in Fig. 3. The SO<sub>2</sub> reduction in Beijing and

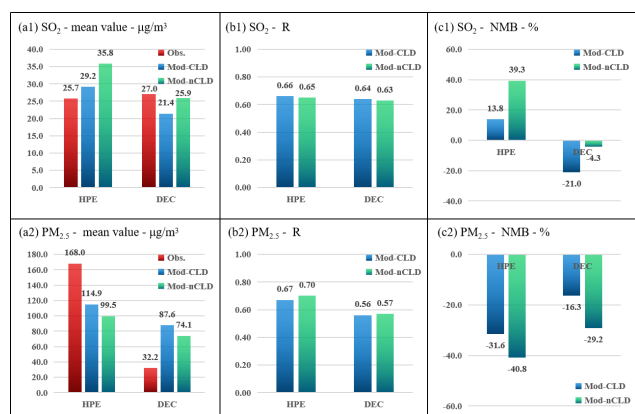


**Figure 12.** Statistical metrics for hourly  $\text{SO}_2$  and  $\text{PM}_{2.5}$  in all selected sites for HPE-2 and DEC with (Mod-CLD) and without (Mod-*n*CLD) cloud chemistry. The mean value (**a1**, unit:  $\mu\text{g m}^{-3}$ ),  $R$  (**b1**), and NMB (**c1**, unit: %) of  $\text{SO}_2$ , as well as the mean value (**a2**, unit:  $\mu\text{g m}^{-3}$ ),  $R$  (**b2**), and NMB (**c2**, unit: %) of  $\text{PM}_{2.5}$ . Obs. denotes the observations.

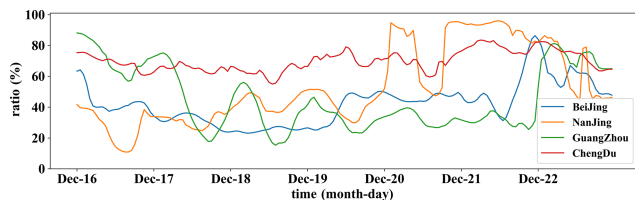


**Figure 13.** The rates of  $\text{SO}_2$  column concentration reduced by cloud chemistry in Beijing (blue), Nanjing (yellow), Guangzhou (green), and Chengdu (red).

Guangzhou was consistently maintained at around 40 % during the period from December 17 to 21. The lower oxidative transformation was related to the lower liquid water content in Beijing, while in Guangzhou it was attributed to the combination of low pollution levels and low cloud water content. Figure 3 shows that Chengdu maintained abundant water vapor conditions from December 17 to 21, as did Nanjing from December 20 to 21. However, the ambient water vapor content was quite low in Guangzhou and Beijing throughout the process and the  $\text{SO}_2$  oxidation was much lower than that of Chengdu and Nanjing. In conclusion, the cloud chemistry process can lead to a  $\text{SO}_2$  column concentration consumption share of more than 60 % when cloud water content is abundant, which is also consistent with the observations of Mount Tai by Li (2020).

The impact of cloud chemistry (RT) on surface  $\text{SO}_2$  and sulfate in four sites is also shown in Fig. 13. The overall trend shows that the peak and valley timing of surface  $\text{SO}_2$  consumption and sulfate increase are coincident. The cloud chemical processes of the surface  $\text{SO}_2$  oxidation vary greatly between cities in different regions (Fig. 14a). In HPE-2, the percentage of surface  $\text{SO}_2$  consumption reached more than 90 % in Chengdu and Nanjing, while it was below 30 % in

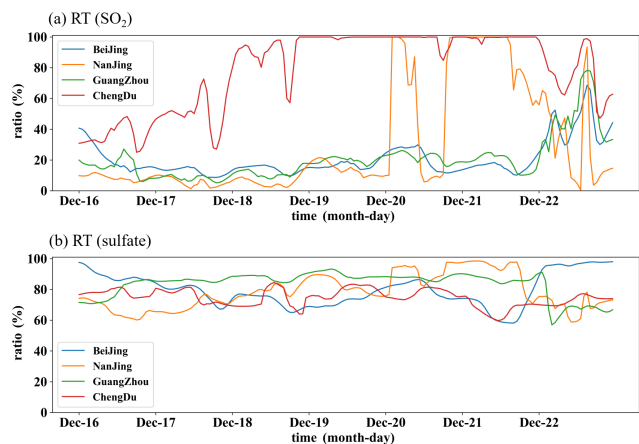


**Figure 14.** The rates of surface  $\text{SO}_2$  reduced (**a**) and the surface sulfate increased (**b**), influenced by cloud chemistry in Beijing (blue), Nanjing (yellow), Guangzhou (green), and Chengdu (red).

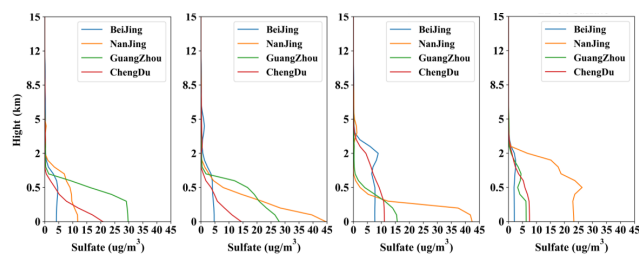


**Figure 15.** Vertical profiles of sulfate concentration difference (DT) at 12:00 on 20 December, at 21:00 on 20 December, at 17:00 on 21 December, and at 12:00 on 22 December in Beijing (blue), Nanjing (yellow), Guangzhou (green), and Chengdu (red).

Beijing and Guangzhou, and did not reach 40 % until December 22. Although the percentage of surface  $\text{SO}_2$  consumption varies greatly, the increase in the percentage of sulfate does not vary much between cities. In HPE-2, the increase in surface sulfate in the four cities ranged from 60 %–95 % (Fig. 14b), which is consistent with the sulfate increase rates summarized by Turnock et al. (2019).

Figure 15 shows the variation of vertical profiles of sulfate increase by the cloud chemistry at the four times of 12:00 LST on 20 December for HPE-2, 04:00 LST on 21 December for HPE-2, and 04:00 and 12:00 LST on 22 December for HPE-3 in Beijing, Nanjing, Chengdu, and Guangzhou. This shows that the sulfate produced by the cloud chemistry during this pollution process is concentrated mostly below 5 km in the troposphere and especially under 2 km. Again, less sulfate has been produced in Beijing in the vertical than that by others by cloud chemistry.

## 4 Summary and conclusions

The cloud chemistry mechanism in WRF/CUACE has been assessed by using the in situ cloud chemistry observations of

SO<sub>2</sub>, O<sub>3</sub>, and H<sub>2</sub>O<sub>2</sub> from Mount Tai in June–July of 2015 and 2018. The results show that the mechanism has well captured the cloud processes for the oxidation of SO<sub>2</sub>, reducing SO<sub>2</sub> by more than 80 % during the cloudy phase, which is in good agreement with the observations.

The cloud chemistry contributions to the changes of SO<sub>2</sub> and sulfate concentrations in NCP, YRD, PRD, and SCB regions are assessed by WRF/CUACE. During heavy pollution (HPE-2), the four regions are significantly affected by cloud chemistry, with SCB being the most obvious. The surface SO<sub>2</sub> reduction in SCB is 1.0–3.0 ppb and reaches 3.0–10.0 ppb in the high value areas, and surface sulfate concentration increased by 10.0–30.0 μg m<sup>-3</sup> on average, with a maximum of more than 20.0–70.0 μg m<sup>-3</sup>. Most areas in NCP, YRD, and PRD have an average SO<sub>2</sub> reduction of 0.5–3.0 ppb and sulfate increase of 5.0–30.0 μg m<sup>-3</sup>. Although the monthly average impact of cloud chemistry is much weaker in the NCP due to less water vapor in December, the contribution in the southern part of NCP during the heavy pollution episode is still significant and cannot be ignored. In PRD, the contribution of cloud chemistry is weaker than other regions due to lighter pollution, although there are many clouds with abundant liquid water there. In addition, the cloud chemistry increases surface sulfate concentrations by 60 %–95 % and reduces surface SO<sub>2</sub> concentrations by more than 80 % in Beijing, Nanjing, Chengdu, and Guangzhou during HPE-2. Above all, the average contribution of cloud chemistry during HPE-2 is significantly greater than that for DEC. Vertically, the cloud chemistry influence is mainly in the middle and lower troposphere below 2 km for four representative cities in HPE-2. Generally, the cloud chemistry can improve the model performance by reducing the overestimates of SO<sub>2</sub> and underestimates of sulfate.

In the future, more mechanisms should be added to improve the cloud chemistry mechanism in CUACE and to increase accuracy in simulating SO<sub>2</sub>, sulfate, and other aerosol components such as nitrate, ammonium, carbonate, and organic aerosols.

**Code and data availability.** All source codes and data can be accessed by contacting the corresponding author Sunling Gong (gongsl@cma.gov.cn).

**Author contributions.** CZ and SG put forward the ideas and formulated the overarching research goals. JL carried them out and wrote the article with suggestions from all authors. LZ and JZ participated in the scientific interpretation and discussion. JC assisted with data acquisition and processing. All authors contributed to the discussion and improvement of the article.

**Competing interests.** The contact author has declared that none of the authors has any competing interests.

**Disclaimer.** Publisher's note: Copernicus Publications remains neutral with regard to jurisdictional claims in published maps and institutional affiliations.

**Review statement.** This paper was edited by Qi Chen and reviewed by two anonymous referees.

**Financial support.** This research has been supported by the National Key Project of the Ministry of Science and Technology of China (grant no. 2022YFC3701205) and the CMA Innovation Development Project (grant no. CXFZ2021J023).

## References

- Alexander, B., Park, R. J., Jacob, D. J., and Gong, S.: Transition metal-catalyzed oxidation of atmospheric sulfur: Global implications for the sulfur budget, *J. Geophys. Res.*, 114, D02309, <https://doi.org/10.1029/2008jd010486>, 2009.
- Binkowski, F. S. and Roselle, S. J.: Models-3 Community Multiscale Air Quality (CMAQ) model aerosol component 1. Model description, *J. Geophys. Res.-Atmos.*, 108, 4183, <https://doi.org/10.1029/2001jd001409>, 2003.
- Buchard, V., da Silva, A. M., Colarco, P., Krotkov, N., Dickerson, R. R., Stehr, J. W., Mount, G., Spinei, E., Arkinson, H. L., and He, H.: Evaluation of GEOS-5 sulfur dioxide simulations during the Frostburg, MD 2010 field campaign, *Atmos. Chem. Phys.*, 14, 1929–1941, <https://doi.org/10.5194/acp-14-1929-2014>, 2014.
- Caffrey, P., Hoppel, W., Frick, G., Pasternack, L., Fitzgerald, J., Hegg, D., Gao, S., Leaitch, R., Shantz, N., Albrechtinski, T., and Ambrusko, J.: In-cloud oxidation of SO<sub>2</sub> by O<sub>3</sub> and H<sub>2</sub>O<sub>2</sub>: Cloud chamber measurements and modeling of particle growth, *J. Geophys. Res.-Atmos.*, 106, 27587–27601, <https://doi.org/10.1029/2000jd900844>, 2001.
- Cao, J., Qiu, X., Gao, J., Wang, F., Wang, J., Wu, J., and Peng, L.: Significant decrease in SO<sub>2</sub> emission and enhanced atmospheric oxidation trigger changes in sulfate formation pathways in China during 2008–2016, *J. Clean. Product.*, 326, 129396, <https://doi.org/10.1016/j.clepro.2021.129396>, 2021.
- Chang, J. S., Brost, R. A., Isaksen, I. S. A., Madronich, S., Middleton, P., Stockwell, W. R., and Walcek, C. J.: A three-dimensional eulerian acid deposition model physical concepts and formulation, *J. Geophys. Res.*, 92, 14681–14700, <https://doi.org/10.1029/jd092id12p14681>, 1987.
- Chapman, E. G., Gustafson Jr., W. I., Easter, R. C., Barnard, J. C., Ghan, S. J., Pekour, M. S., and Fast, J. D.: Coupling aerosol-cloud-radiative processes in the WRF-Chem model: Investigating the radiative impact of elevated point sources, *Atmos. Chem. Phys.*, 9, 945–964, <https://doi.org/10.5194/acp-9-945-2009>, 2009.
- Charlson, R. J., Schwartz, S. E., Hales, J. M., Cess, R. D., Coakley, J. D., Hansen, J. E., and Hofmann, D. J.: Climate forcing by anthropogenic aerosols, *Science*, 255, 423–423, <https://doi.org/10.1126/science.255.5043.423>, 1992.
- Chen, F., and Dudhia, J.: Coupling an advanced land surface-hydrology model with the Penn State-NCAR MM5 modeling system. Part I: Model implementation and sensitivity,

- Mon. Weather Rev., 129, 569–585, [https://doi.org/10.1175/1520-0493\(2001\)129<0587:caalsh>2.0.co;2](https://doi.org/10.1175/1520-0493(2001)129<0587:caalsh>2.0.co;2), 2001.
- Cheng, Y., Zheng, G., Wei, C., Mu, Q., Zheng, B., Wang, Z., Gao, M., Zhang, Q., He, K., and Carmichael, G.: Reactive nitrogen chemistry in aerosol water as a source of sulfate during haze events in China, *Sci. Adv.*, 2, e1601530, <https://doi.org/10.1126/sciadv.1601530>, 2016.
- Chou, M. D., and Suarez, M. J.: An efficient thermal infrared radiation parameterization for use in general circulation models, NASA Tech. Memorandum 104606 – Vol. 3, NASA, Goddard Space Flight Center, Greenbelt, MD, 1994.
- Dovrou, E., Rivera-Rios, J. C., Bates, K. H., and Keutsch, F. N.: Sulfate Formation via Cloud Processing from Isoprene Hydroxyl Hydroperoxides (ISOPOOH), *Environ. Sci. Technol.*, 53, 12476–12484, <https://doi.org/10.1021/acs.est.9b04645>, 2019.
- Emery, C., Tai, E., and Yarwood, G.: Enhanced meteorological modeling and performance evaluation for two Texas ozone episodes, Corpus ID 127579774, *Biology*, 2001.
- Faloon, I., Conley, S. A., Blomquist, B., Clarke, A. D., Kapustin, V., Howell, S., Lenschow, D. H., and Bandy, A. R.: Sulfur dioxide in the tropical marine boundary layer: dry deposition and heterogeneous oxidation observed during the Pacific Atmospheric Sulfur Experiment, *J. Atmos. Chem.*, 63, 13–32, <https://doi.org/10.1007/s10874-010-9155-0>, 2010.
- Fan, D., Ye, Y., and Wang, W.: Air Pollution Control and Public Health: Evidence from “Air Pollution Prevention and Control Action Plan” in China, *Stat. Res.*, 38, 60–74, <https://doi.org/10.19343/j.cnki.11-1302/c.2021.09.005>, 2010.
- Gao, M., Carmichael, G. R., Wang, Y., Ji, D., Liu, Z., and Wang, Z.: Improving simulations of sulfate aerosols during winter haze over Northern China: the impacts of heterogeneous oxidation by NO<sub>2</sub>, *Front. Environ. Sci. Eng.*, 10, 11, <https://doi.org/10.1007/s11783-016-0878-2>, 2016.
- Ge, W., Liu, J., Yi, K., Xu, J., Zhang, Y., Hu, X., Ma, J., Wang, X., Wan, Y., Hu, J., Zhang, Z., Wang, X., and Tao, S.: Influence of atmospheric in-cloud aqueous-phase chemistry on the global simulation of SO<sub>2</sub> in CESM2, *Atmos. Chem. Phys.*, 21, 16093–16120, <https://doi.org/10.5194/acp-21-16093-2021>, 2021.
- Ge, W., Liu, J., Xiang, S., Zhou, Y., Zhou, J., Hu, X., Ma, J., Wang, X., Wan, Y., Hu, J., Zhang, Z., Wang, X., and Tao, S.: Improvement and uncertainties of global simulation of sulfate concentration and radiative forcing in CESM2, *J. Geophys. Res.-Atmos.*, 127, e2022JD037623, <https://doi.org/10.1029/2022JD037623>, 2022.
- Gen, M., Zhang, R., Huang, D. D., Li, Y., and Chan, C. K.: Heterogeneous Oxidation of SO(2) in Sulfate Production during Nitrate Photolysis at 300 nm: Effect of pH, Relative Humidity, Irradiation Intensity, and the Presence of Organic Compounds, *Environ. Sci. Technol.*, 53, 8757–8766, <https://doi.org/10.1021/acs.est.9b01623>, 2019a.
- Gen, M., Zhang, R., Huang, D. D., Li, Y., and Chan, C. K.: Heterogeneous SO<sub>2</sub> Oxidation in Sulfate Formation by Photolysis of Particulate Nitrate, *Environ. Sci. Technol. Lett.*, 6, 86–91, <https://doi.org/10.1021/acs.estlett.8b00681>, 2019b.
- Georgiou, G. K., Christoudias, T., Proestos, Y., Kushta, J., Hadjiniocolaou, P., and Lelieveld, J.: Air quality modelling in the summer over the eastern Mediterranean using WRF-Chem: chemistry and aerosol mechanism intercomparison, *Atmos. Chem. Phys.*, 18, 1555–1571, <https://doi.org/10.5194/acp-18-1555-2018>, 2018.
- Gong, S. L. and Zhang, X. Y.: CUACE/Dust – an integrated system of observation and modeling systems for operational dust forecasting in Asia, *Atmos. Chem. Phys.*, 8, 2333–2340, <https://doi.org/10.5194/acp-8-2333-2008>, 2008.
- Gong, S. L., Barrie, L. A., Blanchet, J. P., von Salzen, K., Lohmann, U., Lesins, G., Spacek, L., Zhang, L. M., Girard, E., Lin, H., Leaitch, R., Leighton, H., Chylek, P., and Huang, P.: Canadian Aerosol Module: A size-segregated simulation of atmospheric aerosol processes for climate and air quality models I. Module development, *J. Geophys. Res.*, 108, 4007, <https://doi.org/10.1029/2001jd002002>, 2003.
- Grell, G. A.: Prognostic evaluation of assumptions used by cumulus parameterizations, *Mon. Weather Rev.*, 121, 764–787, [https://doi.org/10.1175/1520-0493\(1993\)121<0764:peaub>2.0.co;2](https://doi.org/10.1175/1520-0493(1993)121<0764:peaub>2.0.co;2), 1993.
- Guo, J., Wang, Y., Shen, X., Wang, Z., Lee, T., Wang, X., Li, P., Sun, M., Jeffrey, L., Collett, J., Wang, W., and Wang, T.: Characterization of cloud water chemistry at Mount Tai, China: Seasonal variation, anthropogenic impact, and cloud processing, *Atmos. Environ.*, 60, 467–476, [10.1016/j.atmosenv.2012.07.016](https://doi.org/10.1016/j.atmosenv.2012.07.016), 2012.
- Guo, S., Hu, M., Zamora, M. L., Peng, J., Shang, D., Zheng, J., Du, Z., Wu, Z., Shao, M., Zeng, L., Molina, M. J., and Zhang, R.: Elucidating severe urban haze formation in China, *P. Natl. Acad. Sci. USA*, 111, 17373–17378, <https://doi.org/10.1073/pnas.1419604111>, 2014.
- Harris, E., Sinha, B., van Pinxteren, D., Tilgner, A., Fomba, K. W., Schneider, J., Roth, A., Gnauk, T., Fahlbusch, B., Mertes, S., Lee, T., Collett, J., Foley, S., Borrmann, S., Hoppe, P., and Herrmann, H.: Enhanced role of transition metal ion catalysis during in-cloud oxidation of SO<sub>2</sub>, *Science*, 340, 727–730, <https://doi.org/10.1126/science.1230911>, 2013.
- He, J. and Zhang, Y.: Improvement and further development in CESM/CAM5: gas-phase chemistry and inorganic aerosol treatments, *Atmos. Chem. Phys.*, 14, 9171–9200, <https://doi.org/10.5194/acp-14-9171-2014>, 2014.
- He, J., Zhang, Y., Glotfelty, T., He, R., Bennartz, R., Rausch, J., and Sartelet, K.: Decadal simulation and comprehensive evaluation of CESM/CAM5.1 with advanced chemistry, aerosol microphysics, and aerosol-cloud interactions, *J. Adv. Model. Earth Syst.*, 7, 110–141, <https://doi.org/10.1002/2014ms000360>, 2015.
- Hong, C., Zhang, Q., Zhang, Y., Tang, Y., Tong, D., and He, K.: Multi-year downscaling application of two-way coupled WRF v3.4 and CMAQ v5.0.2 over east Asia for regional climate and air quality modeling: model evaluation and aerosol direct effects, *Geosci. Model Dev.*, 10, 2447–2470, <https://doi.org/10.5194/gmd-10-2447-2017>, 2017a.
- Hong, C., Zhang, Q., He, K., Guan, D., Li, M., Liu, F., and Zheng, B.: Variations of China’s emission estimates: response to uncertainties in energy statistics, *Atmos. Chem. Phys.*, 17, 1227–1239, <https://doi.org/10.5194/acp-17-1227-2017>, 2017b.
- Huang, L., An, J., Koo, B., Yarwood, G., Yan, R., Wang, Y., Huang, C., and Li, L.: Sulfate formation during heavy winter haze events and the potential contribution from heterogeneous SO<sub>2</sub> + NO<sub>2</sub> reactions in the Yangtze River Delta region, China, *Atmos. Chem. Phys.*, 19, 14311–14328, <https://doi.org/10.5194/acp-19-14311-2019>, 2019.
- Hung, H. M., Hsu, M. N., and Hoffmann, M. R.: Quantification of SO<sub>2</sub> Oxidation on Interfacial Surfaces of Acidic Micro-Droplets: Implication for Ambient Sulfate Formation, *Environ. Sci. Tech-*

- nol., 52, 9079–9086, <https://doi.org/10.1021/acs.est.8b01391>, 2018.
- Ibusuki, T. and Takeuchi, K.: Sulfur dioxide oxidation by oxygen catalyzed by mixtures of manganese(II) and iron(III) in aqueous solutions at environmental reaction conditions, *Atmos. Environ.*, 21, 1555–1560, [https://doi.org/10.1016/0004-6981\(87\)90317-9](https://doi.org/10.1016/0004-6981(87)90317-9), 1987.
- Ivanova, I. T. and Leighton, H. G.: Aerosol–Cloud Interactions in a Mesoscale Model. Part II: Sensitivity to Aqueous-Phase Chemistry, *J. Atmos. Sci.*, 65, 309–330, <https://doi.org/10.1175/2007jas2276.1>, 2008.
- Janjić, Z. I.: The Step-Mountain Eta Coordinate Model: Further Developments of the Convection, Viscous Sub-layer, and Turbulence Closure, Schemes, *Mon. Weather Rev.*, 122, 927–945, [https://doi.org/10.1175/1520-0493\(1994\)122<0927:tsmecm>2.0.co;2](https://doi.org/10.1175/1520-0493(1994)122<0927:tsmecm>2.0.co;2), 1994.
- Ke, H., Gong, S., He, J., Zhou, C., Zhang, L., and Zhou, Y.: Assessment of Open Biomass Burning Impacts on Surface PM<sub>2.5</sub> Concentration, *Chi. Acad. Meteorol. Sci.*, 31, 105–116, <https://doi.org/10.11898/1001-7313.20200110>, 2020.
- Kong, L., Feng, M., Liu, Y., Zhang, Y., Zhang, C., Li, C., Qu, Y., An, J., Liu, X., Tan, Q., Cheng, N., Deng, Y., Zhai, R., and Wang, Z.: Elucidating the pollution characteristics of nitrate, sulfate and ammonium in PM<sub>2.5</sub> in Chengdu, southwest China, based on 3-year measurements, *Atmos. Chem. Phys.*, 20, 11181–11199, <https://doi.org/10.5194/acp-20-11181-2020>, 2020.
- Kotarba, A. Z.: Calibration of global MODIS cloud amount using CALIOP cloud profiles, *Atmos. Meas. Tech.*, 13, 4995–5012, <https://doi.org/10.5194/amt-13-4995-2020>, 2020.
- Leighton, H. G. and Ivanova, I. T.: Aerosol–Cloud Interactions in a Mesoscale Model. Part I: Sensitivity to Activation and Collision–Coalescence, *J. Atmos. Sci.*, 65, 289–308, <https://doi.org/10.1175/2007jas2207.1>, 2008.
- Lelieveld, J. and Heintzenberg, J.: Sulfate cooling effect on climate through in-cloud oxidation of anthropogenic SO<sub>2</sub>, *Science*, 258, 117–120, <https://doi.org/10.1126/science.258.5079.117>, 1992.
- Li, J.: Microphysical Characteristics and S(IV) Multiphase Chemical Reaction Mechanism of Orographic Clouds, Ph.D. thesis, Department of Environmental Science & Engineering, Fudan University, 113 pp., 2020.
- Li, J., Wang, X., Chen, J., Zhu, C., Li, W., Li, C., Liu, L., Xu, C., Wen, L., Xue, L., Wang, W., Ding, A., and Herrmann, H.: Chemical composition and droplet size distribution of cloud at the summit of Mount Tai, China, *Atmos. Chem. Phys.*, 17, 9885–9896, <https://doi.org/10.5194/acp-17-9885-2017>, 2017.
- Li, J., Zhu, C., Chen, H., Fu, H., Xiao, H., Wang, X., Herrmann, H., and Chen, J.: A More Important Role for the Ozone-S(IV) Oxidation Pathway Due to Decreasing Acidity in Clouds, *J. Geophys. Res.-Atmos.*, 125, e2020JD033220, <https://doi.org/10.1029/2020jd033220>, 2020a.
- Li, J., Zhu, C., Chen, H., Zhao, D., Xue, L., Wang, X., Li, H., Liu, P., Liu, J., Zhang, C., Mu, Y., Zhang, W., Zhang, L., Herrmann, H., Li, K., Liu, M., and Chen, J.: The evolution of cloud and aerosol microphysics at the summit of Mt. Tai, China, *Atmos. Chem. Phys.*, 20, 13735–13751, <https://doi.org/10.5194/acp-20-13735-2020>, 2020b.
- Li, M., Liu, H., Geng, G., Hong, C., Liu, F., Song, Y., Tong, D., Zheng, B., Cui, H., Man, H., Zhang, Q., and He, K.: Anthropogenic emission inventories in China: a review, *Nat. Sci. Rev.*, 4, 834–866, <https://doi.org/10.1093/nsr/nwx150>, 2017.
- Li, P.: Fog Water Chemistry and Fog-Haze Transformation in Shanghai, Ph.D. thesis, Department of Environmental Science & Engineering, Fudan University, 133 pp., 2011.
- Lin, Y. L., Farley, R. D., and Orville, H. D.: Bulk Parameterization of the Snow Field in a Cloud Model, *J. Appl. Meteorol.*, 22, 1065–1092, [https://doi.org/10.1175/1520-0450\(1983\)022<1065:bpotsf>2.0.co;2](https://doi.org/10.1175/1520-0450(1983)022<1065:bpotsf>2.0.co;2), 1983.
- Liu, S. C., McKeen, S. A., Hsie, E. Y., Lin, X., Kelly, K. K., Bradshaw, J. D., Sandholm, S. T., Browell, E. V., Gregory, G. L., Sachse, G. W., Bandy, A. R., Thornton, D. C., Blake, D. R., Rowland, F. S., Newell, R., Heikes, B. G., Singh, H., and Talbot, R. W.: Model study of tropospheric trace species distributions during PEM-WEST A, *J. Geophys. Res.*, 101, 2073–2085, <https://doi.org/10.1029/95JD02277>, 1996.
- Liu, T., Chan, A. W. H., and Abbatt, J. P. D.: Multiphase Oxidation of Sulfur Dioxide in Aerosol Particles: Implications for Sulfate Formation in Polluted Environments, *Environ. Sci. Technol.*, 55, 4227–4242, <https://doi.org/10.1021/acs.est.0c06496>, 2021.
- Lu, X., Zhang, S., Xing, J., Wang, Y., Chen, W., Ding, D., Wu, Y., Wang, S., Duan, L., and Hao, J.: Progress of Air Pollution Control in China and Its Challenges and Opportunities in the Ecological Civilization Era, *Engineering*, 6, 1423–1431, <https://doi.org/10.1016/j.eng.2020.03.014>, 2020.
- Maahs, H. G.: Kinetics and Mechanism of the Oxidation of S(IV) by Ozone in Aqueous Solution With Particular Reference to SO<sub>2</sub> Conversion in Nonurban Tropospheric Clouds, *J. Geophys. Res.-Oceans*, 88, 10721–10732, <https://doi.org/10.1029/JC088iC15p10721>, 1983.
- Martin, G. M., Johnson D. W., and Spice A.: The measurement and parameterization of effective radius in warm stratocumulus cloud, *J. Atmos. Sci.*, 51, 1823–1842, [https://doi.org/10.1175/1520-0469\(1994\)051<1823:TMAPOE>2.0.CO;2](https://doi.org/10.1175/1520-0469(1994)051<1823:TMAPOE>2.0.CO;2), 1994.
- Martin, L. R. and Good, T. W.: Catalyzed oxidation of sulfur dioxide in solution: The iron-manganese synergism, *Atmos. Environ.*, 25, 2395–2399, [https://doi.org/10.1016/0960-1686\(91\)90113-L](https://doi.org/10.1016/0960-1686(91)90113-L), 1991.
- Menut, L., Bessagnet, B., Khvorostyanov, D., Beekmann, M., Blond, N., Colette, A., Coll, I., Curci, G., Foret, G., Hodzic, A., Mailler, S., Meleux, F., Monge, J.-L., Pison, I., Siour, G., Turquety, S., Valari, M., Vautard, R., and Vivanco, M. G.: CHIMERE 2013: a model for regional atmospheric composition modelling, *Geosci. Model Dev.*, 6, 981–1028, <https://doi.org/10.5194/gmd-6-981-2013>, 2013.
- Mlawer, E. J., Taubman, S. J., Brown, P. D., Iacono, M. J., and Clough, S. A.: Radiative transfer for inhomogeneous atmospheres: RRTM, a validated correlated-k model for the longwave, *J. Geophys. Res. -Atmos.*, 102, 16663–16682, <https://doi.org/10.1029/97jd00237>, 1997.
- Moch, J. M., Dovrou, E., Mickley, L. J., Keutsch, F. N., Cheng, Y., Jacob, D. J., Jiang, J., Li, M., Munger, J. W., Qiao, X., and Zhang, Q.: Contribution of Hydroxymethane Sulfonate to Ambient Particulate Matter: A Potential Explanation for High Particulate Sulfur During Severe Winter Haze in Beijing, *Geophys. Res. Lett.*, 45, 11969–11979, <https://doi.org/10.1029/2018gl079309>, 2018.

- Molina: Air Quality in the Mexico Megacity: An Integrated Assessment, *All. Glo. Sus.*, 2, 141–145, <https://doi.org/10.1007/978-94-010-0454-1>, 2002.
- Park, R. J. and Jacob, D. J.: Sources of carbonaceous aerosols over the United States and implications for natural visibility, *J. Geophys. Res.*, 108, 4355, <https://doi.org/10.1029/2002jd003190>, 2003.
- Peng, J., Hu, M., Shang, D., Wu, Z., Du, Z., Tan, T., Wang, Y., Zhang, F., and Zhang, R.: Explosive Secondary Aerosol Formation during Severe Haze in the North China Plain, *Environ. Sci. Technol.*, 55, 2189–2207, <https://doi.org/10.1021/acs.est.0c07204>, 2021.
- Pye, H. O. T., Nenes, A., Alexander, B., Ault, A. P., Barth, M. C., Clegg, S. L., Collett Jr., J. L., Fahey, K. M., Hennigan, C. J., Herrmann, H., Kanakidou, M., Kelly, J. T., Ku, I.-T., McNeill, V. F., Riemer, N., Schaefer, T., Shi, G., Tilgner, A., Walker, J. T., Wang, T., Weber, R., Xing, J., Zaveri, R. A., and Zuend, A.: The acidity of atmospheric particles and clouds, *Atmos. Chem. Phys.*, 20, 4809–4888, <https://doi.org/10.5194/acp-20-4809-2020>, 2020.
- Ramanathan, V., Crutzen, P. J., Kiehl, J. T., and Rosenfeld, D.: Aerosols, climate, and the hydrological cycle, *Science*, 294, 2119–2124, [10.1126/science.1064034](https://doi.org/10.1126/science.1064034), 2001.
- Ravishankara, A. R.: Heterogeneous and Multiphase Chemistry in the Troposphere, *Science*, 276, 1058–1065, <https://doi.org/10.1126/science.276.5315.1058>, 1997.
- Ren, Y., Ding, A., Wang, T., Shen, X., Guo, J., Zhang, J., Wang, Y., Xu, P., Wang, X., and Gao, J.: Measurement of gas-phase total peroxides at the summit of Mount Tai in China, *Atmos. Environ.*, 43, 1702–1711, <https://doi.org/10.1016/j.atmosenv.2008.12.020>, 2009.
- Sha, T., Ma, X., Jia, H., Tian, R., Chang, Y., Cao, F., and Zhang, Y.: Aerosol chemical component: Simulations with WRF-Chem and comparison with observations in Nanjing, *Atmos. Environ.*, 218, 116982, <https://doi.org/10.1016/j.atmosenv.2019.116982>, 2019a.
- Sha, T., Ma, X., Jia, H., van der A, R. J., Ding, J., Zhang, Y., and Chang, Y.: Exploring the influence of two inventories on simulated air pollutants during winter over the Yangtze River Delta, *Atmos. Environ.*, 206, 170–182, <https://doi.org/10.1016/j.atmosenv.2019.03.006>, 2019b.
- Shen, X., Lee, T., Guo, J., Wang, X., Li, P., Xu, P., Wang, Y., Ren, Y., Wang, W., Wang, T., Li, Y., Carn, S. A., and Collett, J. L.: Aqueous phase sulfate production in clouds in eastern China, *Atmos. Environ.*, 62, 502–511, <https://doi.org/10.1016/j.atmosenv.2012.07.079>, 2012.
- Sielski, J., Kazirod-Wolski, K., Jozwiak, M. A., and Jozwiak, M.: The influence of air pollution by PM<sub>2.5</sub>, PM<sub>10</sub> and associated heavy metals on the parameters of out-of-hospital cardiac arrest, *Sci. Total Environ.*, 788, 147541, <https://doi.org/10.1016/j.scitotenv.2021.147541>, 2021.
- Song, S., Gao, M., Xu, W., Sun, Y., Worsnop, D. R., Jayne, J. T., Zhang, Y., Zhu, L., Li, M., Zhou, Z., Cheng, C., Lv, Y., Wang, Y., Peng, W., Xu, X., Lin, N., Wang, Y., Wang, S., Munger, J. W., Jacob, D. J., and McElroy, M. B.: Possible heterogeneous chemistry of hydroxymethanesulfonate (HMS) in northern China winter haze, *Atmos. Chem. Phys.*, 19, 1357–1371, <https://doi.org/10.5194/acp-19-1357-2019>, 2019.
- Sun, K., Liu, H., Ding, A., and Wang, X.: WRF-Chem Simulation of a Severe Haze Episode in the Yangtze River Delta, China, *Aerosol Air Qual. Res.*, 16, 1268–1283, <https://doi.org/10.4209/aaqr.2015.04.0248>, 2016.
- Terrenoire, E., Bessagnet, B., Rouil, L., Tognet, F., Pirovano, G., Létinois, L., Beauchamp, M., Colette, A., Thunis, P., Amann, M., and Menut, L.: High-resolution air quality simulation over Europe with the chemistry transport model CHIMERE, *Geosci. Model Dev.*, 8, 21–42, <https://doi.org/10.5194/gmd-8-21-2015>, 2015.
- Tie, X.: Assessment of the global impact of aerosols on tropospheric oxidants, *J. Geophys. Res.*, 110, D03204, <https://doi.org/10.1029/2004jd005359>, 2005.
- Tuccella, P., Curci, G., Visconti, G., Bessagnet, B., Menut, L., and Park, R. J.: Modeling of gas and aerosol with WRF/Chem over Europe: Evaluation and sensitivity study, *J. Geophys. Res.*, 117, D03303, <https://doi.org/10.1029/2011JD016302>, 2012.
- Turnock, S. T., Mann, G. W., Woodhouse, M. T., Dalvi, M., O'Connor, F. M., Carslaw, K. S., and Sprackle, D. V.: The Impact of Changes in Cloud Water pH on Aerosol, *Geophys. Res. Lett.*, 46, 4039–4048, [10.1029/2019GL082067](https://doi.org/10.1029/2019GL082067), 2019.
- Twomey, S.: Aerosols, clouds and radiation, *Atmospheric Environment, part A, general Topics*, 25, 2435–2442, [https://doi.org/10.1016/0960-1686\(91\)90159-5](https://doi.org/10.1016/0960-1686(91)90159-5), 1991.
- Twomey, S. A., Piepgrass, M., and Wolfe, T. L.: An assessment of the impact of pollution on the global cloud albedo, *Tellus B*, 36B, 356–366, <https://doi.org/10.1111/j.1600-0889.1984.tb00254.x>, 1984.
- von Salzen, K., Leighton, H. G., Ariya, P. A., Barrie, L. A., Gong, S. L., Blanchet, J. P., Spacek, L., Lohmann, U., and Kleinman, L. I.: Sensitivity of sulphate aerosol size distributions and CCN concentrations over North America to SO<sub>x</sub> emissions and H<sub>2</sub>O<sub>2</sub> concentrations, *J. Geophys. Res.-Atmos.*, 105, 9741–9765, <https://doi.org/10.1029/2000jd900027>, 2000.
- Wang, G., Zhang, R., Gomez, M. E., Yang, L., Levy Zamora, M., Hu, M., Lin, Y., Peng, J., Guo, S., Meng, J., Li, J., Cheng, C., Hu, T., Ren, Y., Wang, Y., Gao, J., Cao, J., An, Z., Zhou, W., Li, G., Wang, J., Tian, P., Marrero-Ortiz, W., Secret, J., Du, Z., Zheng, J., Shang, D., Zeng, L., Shao, M., Wang, W., Huang, Y., Wang, Y., Zhu, Y., Li, Y., Hu, J., Pan, B., Cai, L., Cheng, Y., Ji, Y., Zhang, F., Rosenfeld, D., Liss, P. S., Duce, R. A., Kolb, C. E., and Molina, M. J.: Persistent sulfate formation from London Fog to Chinese haze, *P. Natl. Acad. Sci. USA*, 113, 13630–13635, <https://doi.org/10.1073/pnas.1616540113>, 2016.
- Wang, H., Shi, G. Y., Zhang, X. Y., Gong, S. L., Tan, S. C., Chen, B., Che, H. Z., and Li, T.: Mesoscale modelling study of the interactions between aerosols and PBL meteorology during a haze episode in China Jing-Jin-Ji and its near surrounding region – Part 2: Aerosols' radiative feedback effects, *Atmos. Chem. Phys.*, 15, 3277–3287, <https://doi.org/10.5194/acp-15-3277-2015>, 2015.
- Wang, J., Li, J., Ye, J., Zhao, J., Wu, Y., Hu, J., Liu, D., Nie, D., Shen, F., Huang, X., Huang, D. D., Ji, D., Sun, X., Xu, W., Guo, J., Song, S., Qin, Y., Liu, P., Turner, J. R., Lee, H. C., Hwang, S., Liao, H., Martin, S. T., Zhang, Q., Chen, M., Sun, Y., Ge, X., and Jacob, D. J.: Fast sulfate formation from oxidation of SO<sub>2</sub> by NO<sub>2</sub> and HONO observed in Beijing haze, *Nat. Commun.*, 11, 2844, <https://doi.org/10.1038/s41467-020-16683-x>, 2020.
- Wang, S., Zhou, S., Tao, Y., Tsui, W. G., Ye, J., Yu, J. Z., Murphy, J. G., McNeill, V. F., Abbatt, J. P. D., and Chan, A. W. H.: Organic Peroxides and Sulfur Dioxide in Aerosol: Source

- of Particulate Sulfate, *Environ. Sci. Technol.*, 53, 10695–10704, <https://doi.org/10.1021/acs.est.9b02591>, 2019.
- Wang, T., Liu, M., Liu, M., Song, Y., Xu, Z., Shang, F., Huang, X., Liao, W., Wang, W., Ge, M., Cao, J., Hu, J., Tang, G., Pan, Y., Hu, M., and Zhu, T.: Sulfate Formation Apportionment during Winter Haze Events in North China, *Environ. Sci. Technol.*, 56, 7771–7778, <https://doi.org/10.1021/acs.est.2c02533>, 2022.
- Wang, W., Liu, M., Wang, T., Song, Y., Zhou, L., Cao, J., Hu, J., Tang, G., Chen, Z., Li, Z., Xu, Z., Peng, C., Lian, C., Chen, Y., Pan, Y., Zhang, Y., Sun, Y., Li, W., Zhu, T., Tian, H., and Ge, M.: Sulfate formation is dominated by manganese-catalyzed oxidation of SO(2) on aerosol surfaces during haze events, *Nat. Commun.*, 12, 1993, <https://doi.org/10.1038/s41467-021-22091-6>, 2021.
- Wang, Y., Zhang, Q. Q., Jiang, J., Zhou, W., Wang, B., He, K., Duan, F., Zhang, Q., Philip, S., and Xie, Y.: Enhanced sulfate formation during China's severe winter haze episode in January 2013 missing from current models, *J. Geophys. Res.-Atmos.*, 119, 10425–10440, <https://doi.org/10.1002/2013JD021426>, 2014.
- Wei, Y., Chen, X., Chen, H., Li, J., Wang, Z., Yang, W., Ge, B., Du, H., Hao, J., Wang, W., Li, J., Sun, Y., and Huang, H.: IAP-AACM v1.0: a global to regional evaluation of the atmospheric chemistry model in CAS-ESM, *Atmos. Chem. Phys.*, 19, 8269–8296, <https://doi.org/10.5194/acp-19-8269-2019>, 2019.
- Xie, Y., Dai, H., Zhang, Y., Wu, Y., Hanaoka, T., and Masui, T.: Comparison of health and economic impacts of PM<sub>2.5</sub> and ozone pollution in China, *Environ. Int.*, 130, 104881, <https://doi.org/10.1016/j.envint.2019.05.075>, 2019.
- Yao, M., Zhao, Y., Hu, M., Huang, D., Wang, Y., Yu, J. Z., and Yan, N.: Multiphase Reactions between Secondary Organic Aerosol and Sulfur Dioxide: Kinetics and Contributions to Sulfate Formation and Aerosol Aging, *Environ. Sci. Technol. Lett.*, 6, 768–774, <https://doi.org/10.1021/acs.estlett.9b00657>, 2019.
- Yao, S., Wang, Q., Zhang, J., and Zhang, R.: Characteristics of Aerosol and Effect of Aerosol-Radiation-Feedback in Handan, an Industrialized and Polluted City in China in Haze Episodes, *Atmosphere*, 12, 670, <https://doi.org/10.3390/atmos12060670>, 2021.
- Ye, C., Xue, C., Zhang, C., Ma, Z., Liu, P., Zhang, Y., Liu, C., Zhao, X., Zhang, W., He, X., Song, Y., Liu, J., Wang, W., Sui, B., Cui, R., Yang, X., Mei, R., Chen, J., and Mu, Y.: Atmospheric Hydrogen Peroxide H<sub>2</sub>O<sub>2</sub> at the Foot and Summit of Mt Tai Variations Sources, *J. Geophys. Res.-Atmos.*, 126, e2020JD033975, <https://doi.org/10.1029/2020JD033975>, 2021.
- Ye, J., Abbatt, J. P. D., and Chan, A. W. H.: Novel pathway of SO<sub>2</sub> oxidation in the atmosphere: reactions with monoterpene ozonolysis intermediates and secondary organic aerosol, *Atmos. Chem. Phys.*, 18, 5549–5565, <https://doi.org/10.5194/acp-18-5549-2018>, 2018.
- Zhang, L., Gong, S., Zhao, T., Zhou, C., Wang, Y., Li, J., Ji, D., He, J., Liu, H., Gui, K., Guo, X., Gao, J., Shan, Y., Wang, H., Wang, Y., Che, H., and Zhang, X.: Development of WR-F/CUACE v1.0 model and its preliminary application in simulating air quality in China, *Geosci. Model Dev.*, 14, 703–718, <https://doi.org/10.5194/gmd-14-703-2021>, 2021.
- Zhang, X. Y., Wang, Y. Q., Niu, T., Zhang, X. C., Gong, S. L., Zhang, Y. M., and Sun, J. Y.: Atmospheric aerosol compositions in China: spatial/temporal variability, chemical signature, regional haze distribution and comparisons with global aerosols, *Atmos. Chem. Phys.*, 12, 779–799, <https://doi.org/10.5194/acp-12-779-2012>, 2012.
- Zheng, B., Tong, D., Li, M., Liu, F., Hong, C., Geng, G., Li, H., Li, X., Peng, L., Qi, J., Yan, L., Zhang, Y., Zhao, H., Zheng, Y., He, K., and Zhang, Q.: Trends in China's anthropogenic emissions since 2010 as the consequence of clean air actions, *Atmos. Chem. Phys.*, 18, 14095–14111, <https://doi.org/10.5194/acp-18-14095-2018>, 2018.
- Zhou, C., Zhang, X., Zhang, J., and Zhang, X.: Representations of dynamics size distributions of mineral dust over East Asia by a regional sand and dust storm model, *Atmos. Res.*, 250, 18965, <https://doi.org/10.1016/j.atmosres.2020.105403>, 2021.
- Zhou, C., Zhang, X., Gong, S., Wang, Y., and Xue, M.: Improving aerosol interaction with clouds and precipitation in a regional chemical weather modeling system, *Atmos. Chem. Phys.*, 16, 145–160, <https://doi.org/10.5194/acp-16-145-2016>, 2016.
- Zhou, C. H., Gong, S., Zhang, X. Y., Liu, H. L., Xue, M., Cao, G. L., An, X. Q., and Che, H. Z.: Towards the improvements of simulating the chemical and optical properties of Chinese aerosols using an online coupled model – CUACE/Aero, *Tellus B*, 64, 18965, <https://doi.org/10.3402/tellusb.v64i0.18965>, 2012.
- Zhou, Y., Gong, S., Zhou, C., Zhang, L., He, J., Wang, Y., Ji, D., Feng, J., Mo, J., and Ke, H.: A new parameterization of uptake coefficients for heterogeneous reactions on multi-component atmospheric aerosols, *Sci. Total Environ.*, 781, 146372, <https://doi.org/10.1016/j.scitotenv.2021.146372>, 2021.
- Zhu, Y., Yang, L., Chen, J., Kawamura, K., Sato, M., Tilgner, A., van Pinxteren, D., Chen, Y., Xue, L., Wang, X., Simpson, I. J., Herrmann, H., Blake, D. R., and Wang, W.: Molecular distributions of dicarboxylic acids, oxocarboxylic acids and  $\alpha$ -dicarbonyls in PM<sub>2.5</sub> collected at the top of Mt. Tai, North China, during the wheat burning season of 2014, *Atmos. Chem. Phys.*, 18, 10741–10758, <https://doi.org/10.5194/acp-18-10741-2018>, 2018.